

# Chapter 1

## Pulsed Field Gradient—NMR Sequences

**Abstract** The mechanism via which an NMR signal is generated and how diffusion can be measured from solving the equation of motion of the nuclear spins is described. A set of basic pulsed field gradient (PFG) NMR sequences are provided, along with their corresponding echo attenuations. The concept of spin echoes is given along with a description of coherence transfer pathways, a tool for acquiring the wanted spin echo signal. Two Mathematica programs are provided, which describe a calculation necessary in order to produce diffusion coefficients from PFG NMR experiments using quadratic and sinusoidal gradients.

The pulsed field gradient (PFG) nuclear magnetic resonance (NMR) method is a well-established technique for studying molecular motion without disturbing the system under investigation [1–17]. It could be described as a non-invasive approach, as the only perturbation performed on the system is to alter the phase and/or the direction of the nuclear magnetic moments of the diffusing molecules in order to get a detectable signal [18–20]. A large variety of diffusion weighted sequences or techniques have been proposed that are optimised for different tasks, such as diffusion measurements in the presence of internal magnetic field gradients induced due to magnetic susceptibility changes through the sample, convection within the sample, or large eddy current field transients arising from any conducting metal surrounding the sample. This variety of PFG sequences not only reflects the increasing interest in using the PFG NMR technique in diffusion studies, but also shows that it is not necessarily a trivial task to extract the true diffusion coefficient from a PFG NMR experiment. In the following section, the mechanism via which an NMR signal is generated and how diffusion can be measured from solving the equation of motion of the nuclear spins will be described. Then a set of basic PFG sequences will be provided, along with their corresponding echo attenuations. In the appendix to this section, the concept of spin echoes is discussed along with a description of coherence transfer pathways, a tool for acquiring the wanted spin echo signal. Two Mathematica programs can also be found in the appendix to this chapter, which describe a calculation necessary in order to produce diffusion coefficients from PFG NMR experiments using

quadratic and sinusoidal gradients. An elaborate treatment of the NMR-theory can be found in the book by Slichter [21]

When placing hydrogen or another NMR active nuclei in an external magnetic field, the nuclear magnetic moment will align along the direction of this field. The Hamiltonian for non-interacting nuclear magnetic spins in an external magnetic field can be written [21]

$$\mathbf{H}(t) = -\gamma \hbar \vec{I} \cdot \vec{H}(t) \quad (1.1)$$

$\gamma$  = gyromagnetic ratio (which varies depending on the nucleus under investigation),  $\hbar$  = Planck's constant,  $\vec{I}$  = spin operator and  $\vec{H}(t)$  = external magnetic field. The time dependency of  $\vec{H}(t)$  is included in order to make (1.1) valid when the system is influenced by an oscillating magnetic field (RF-field) and magnetic field gradients (g). When the magnetic field,  $\vec{H}(t)$ , is constant and homogeneous ( $= H_0$ ), the eigenvalues, the energy levels, of a nucleus with  $I = 1/2$  (as in the case of the hydrogen) may be written

$$E = \pm \frac{1}{2} \gamma \hbar H_0 = \pm \frac{1}{2} \hbar \omega_0 \quad (1.2)$$

The difference between the two energy levels is written

$$\Delta E = \hbar \omega_0 \quad (1.3)$$

In thermal equilibrium a difference in population between upper and lower level is given by the Boltzmann factor

$$\frac{n_{upper}}{n_{lower}} = e^{-\frac{\hbar \omega}{kT}} \quad (1.4)$$

$T$  = absolute temperature and  $k$  = Boltzmann's constant. The difference in population will generate a net nuclear magnetic moment, which has an amplitude directly proportional to the number of nuclear spins present in the sample. In thermal equilibrium, the moment will be aligned with the external magnetic field  $H_0$ . By imposing an oscillating magnetic field, RF-field, transverse to the external magnetic field, transitions between the energy levels will occur. The direction of the net nuclear magnetic moment will then move away from alignment with the external field, i.e. thermal equilibrium. When the RF-field is switched off, the system will again tend to align with the external field, the direction of  $H_0$ . The rate back to thermal equilibrium given by the characteristic relaxation times  $T_1$  (longitudinal relaxation) and  $T_2$  (transverse relaxation) represent the rate of loss of coherence in the plane transverse to the external magnetic field. The return to thermal equilibrium in combination with an oscillating net nuclear magnetic moment transverse to  $H_0$  will cause changes in the magnetic flux, which can be recorded with the same RF-coil as was used to excite the system. The concept of generating an NMR spin echo and a gradient spin echo signal is described in Appendix.

## 1.1 The Pulsed Field Gradient (PFG) Diffusion Experiment

A basic PFG stimulated echo sequence shown in Fig. 1.2 consists of 3 intervals, a prepare, a store, and a read interval. In the prepare interval the molecules are labelled with a phase proportional to the integral of the effective gradient  $g(t)$ . In Fig. 1.1 the anti-helmholtz gradient coil is shown, and with proper dimensions on this coil, a linear gradient is generated (Chap. 3)

$$\vec{H}(t) = \vec{H}_0 + g(t) \cdot z \quad (1.5)$$

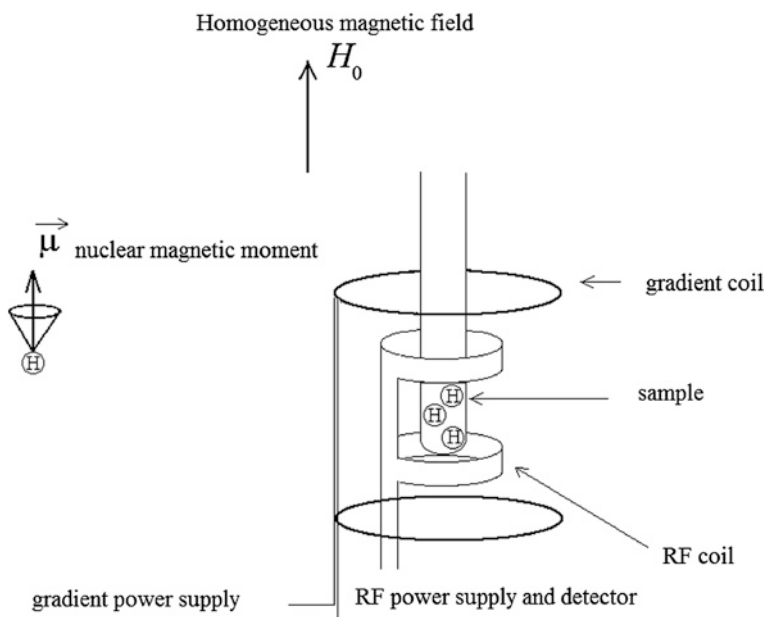


**Fig. 1.1** A schematic drawing of the basics needed for performing a PFG-NMR experiment

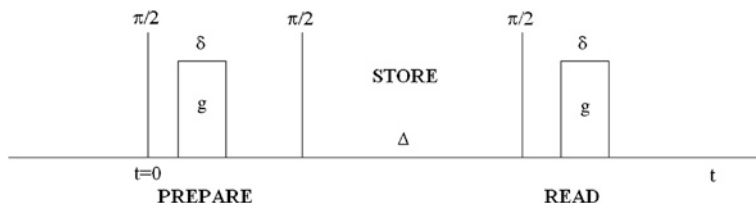


**Fig. 1.2** The PFGSTE sequence where the PREPARE interval labels the phase of the spins, the STORE interval allow the spins to diffuse, and the READ interval labels the spins with a phase of opposite polarity

$z$  is the position of the molecule along the direction of the magnetic field gradient, which again is collinear with  $H_0$  or the longitudinal direction. The mobility of the hydrogen may be recorded by making use of this magnetic field gradient  $g$ , which imposes a position dependent frequency on the system, and with which the nuclear magnetic moment of the proton is oscillating in a plane transverse to  $H_0$

$$\omega = \gamma H_0 + \gamma g z \quad (1.6)$$

After the application of the second pulse, the net magnetic moment is stored in the longitudinal direction, and is thus unaffected by the presence of any transverse relaxation. In the read interval the nuclear spins are labelled with a phase of opposite polarity to the prepare interval. If the molecules have travelled a distance during the PFG-sequence, there is a dephasing of the net magnetic moment given by

$$\Delta\phi = \gamma g(z_2 - z_1) \quad (1.7)$$

$(z_2 - z_1)$  is the distance travelled by the spins in one dimension, during the store interval, when assuming infinitely short gradient pulses. The induced current in the RF coil will be attenuated because of the dephasing. This will be apparent in the pulsed field gradient stimulated echo attenuation expressed as a function of the diffusion time and the gradient strength. In order to calculate the echo attenuation arising from an arbitrary PFG NMR experiment the Bloch equations [20] for a system of diffusing and interacting spins needs to be solved. By imposing a radio frequency field on a proton system situated in an external magnetic field, one may induce transitions between the energy levels, i.e. bringing the system out of thermal equilibrium. Assuming that the spins are interacting and diffusing in the presence of an external magnetic field the classical equation of motion of the spin system is known as the Bloch-Torrey equations in [20, 22]

$$\frac{d}{dt} \vec{M} = \gamma \vec{M} \times \vec{H} + D \nabla^2 \vec{M} \quad (1.8)$$

Equation (1.8) may be written as

$$\begin{aligned} \frac{d}{dt} M_z &= -\gamma M_y H_1 + \frac{M_0 - M_z}{T_1} + D \nabla^2 M_z \\ \frac{d}{dt} M_x &= \gamma M_y h_0 - \frac{M_x}{T_2} + D \nabla^2 M_x \\ \frac{d}{dt} M_y &= \gamma (M_z H_1 - M_x h_0) - \frac{M_y}{T_2} + D \nabla^2 M_y \end{aligned} \quad (1.9)$$

$H_1$  is the rotating magnetic field with a frequency  $\omega$ ,  $h_0 = H_0 + \omega/\gamma$ ,  $T_1$  is the longitudinal or spin lattice relaxation time,  $T_2$  is the transverse or spin-spin relaxation time, and  $D$  is the diffusion coefficient. The acquisition of the NMR signal is performed by sampling the induced magnetic moment in the transverse plane to the external field, and the phases for the transverse components are affected by diffusion in the presence of a magnetic field gradient. During the  $z$ -storage of the net

magnetisation, there is no effect from diffusion in the presence of magnetic field gradients on the net magnetisation. When assuming a Gaussian diffusion propagator [23] and a mono-exponential attenuation of the NMR signal due to relaxation processes, it can be shown that the solution to the transverse magnetisation ( $M^+ = M_x + i M_y$ ) for an arbitrary pulsed field gradient sequence is written [1]

$$M^+ = M_0^+ e^{-\frac{t_1}{T_2}} e^{-\frac{t_2}{T_1}} e^{-\gamma^2 D \int_0^t \left( \int_0^{t'} g(t'') dt'' \right)^2 dt'} \quad (1.10)$$

$M_0^+$  is the integration constant depending on the initial conditions. The applied gradients in (1.10) are the effective gradients. That is, depending on the coherence transfer pathway, the polarity of the gradient may have to be changed after application of a  $180^\circ$  RF-pulse or two  $90^\circ$  RF-pulses (see Appendix or [1]). In the following,  $M^+$  and  $M_0^+$  will be denoted  $I$  and  $I_0$  respectively. The induced current in the RF coil, the NMR signal, will be attenuated because of the dephasing. This will be apparent in the pulsed field gradient stimulated echo attenuation expressed as a function of the diffusion time and the gradient strength.

$$I = I_0 e^{-\frac{t_1}{T_2}} e^{-\frac{t_2}{T_1}} e^{-\gamma^2 D \int_0^t \left( \int_0^{t'} g(t'') dt'' \right)^2 dt'} \quad (1.11)$$

where

- $t_1$  duration during which the NMR-signal is influenced by transverse relaxation processes
- $t_2$  duration during which the NMR-signal is influenced by longitudinal relaxation processes
- $g(t'')$  total effective magnetic field gradient, external and internal
- $D$  diffusion coefficient
- $T_1$  Characteristic longitudinal relaxation time
- $T_2$  Characteristic transverse relaxation time
- $I_0$  Initial intensity of the NMR-signal

The usual way to conduct the diffusion experiment is to fix the durations and vary the applied magnetic field gradients, so that the reduction of the NMR echo signal due to transverse and longitudinal relaxation processes will be constant during the experiment. A general expression for the amplitude of echo signal can then be written

$$I = I_0 e^{-\gamma^2 D \int_0^t \left( \int_0^{t'} g(t'') dt'' \right)^2 dt'} \quad (1.12)$$

In the following discussion, focus will be on the PFG NMR sequences where the diffusion coefficient is measured by generating an attenuated NMR signal by incrementing the applied gradient strength,  $g$ . The two relaxation terms containing  $t_1$  and  $t_2$  become constant and can be incorporated to the initial intensity of

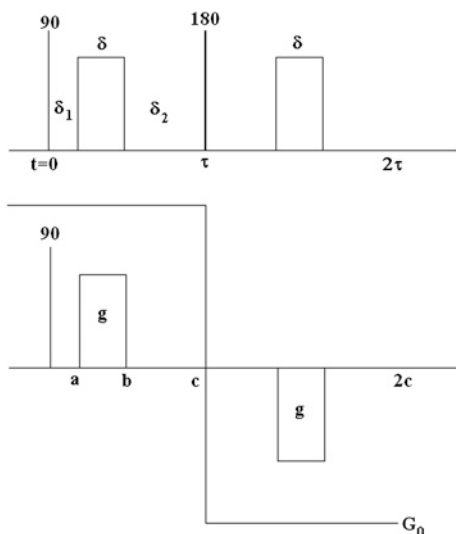
the NMR signal,  $I_0$ , as shown in (1.12). When incrementing the gradient strength and keeping the durations fixed, the diffusing molecules will probe the restrictions of a heterogeneous sample to the same degree during the NMR experiment. The measured diffusion coefficient will then represent a stable system with the respect to the fraction of molecules experiencing the heterogeneity of the sample. This is important when measuring physical parameters such as tortuosity, surface to volume ratio or surface relaxation in heterogeneous media [24–31] (Chap. 2).

Many PFG NMR experiments now combine diffusion measurements with relaxation or spectral measurements [11, 32]. Before showing some basic two-dimensional sequences, the spoiler recovery sequence is introduced. This sequence is designed to circumvent the need for waiting five times the longitudinal relaxation time between each scan while maintaining quantitative diffusion information, and may reduce the experimental time by  $\sim 80\%$  without any significant loss in signal to noise ratio. This method also reduces the impact from radiation damping, so its applicability is for any operating magnetic field, at least in the region 0.05–14.1 T (Chap. 6).

## 1.2 The Ordinary PFGSE Sequence

In Fig. 1.3 the simplest form of the NMR diffusion experiment is shown, the pulsed field gradient spin echo method. This sequence was introduced by Stejskal and Tanner in 1965 [33], and consists of a  $90^\circ$  excitation RF pulse and two mono polar gradient pulses separated by a  $180^\circ$  refocusing RF-pulse. As can be seen in Fig. 1.3 the impact of the refocusing  $180^\circ$  RF-pulse is to change the polarity of the effective gradient. This is a consequence of the impact the RF-pulse has on the evolving

**Fig. 1.3** The pulsed field gradient spin echo (PFGSE) with real (*upper sequence*) and effective gradients (*lower sequence*)



Hamiltonian when calculating the expectation value for the net nuclear magnetization (see Appendix). In order to evaluate the attenuation arising from the sequence it is taken into account that the system is subjected to transverse relaxation processes during the entire sequence. When assuming a Gaussian diffusion propagator, (1.12) can be applied to calculate the effective gradient seen by the nuclear spin system at each particular time interval as shown in column two in Table 1.1. Then the effective gradients for the successive time intervals are integrated, for which results are shown in column three in Table 1.1.

The next step is then to integrate the square of these terms, and the result of this rather tedious calculation even for the simplest PFG sequence is shown for each term in column four (Table 1.2).

**Table 1.1** Column 1 is the time parameter with its corresponding effective gradients in column 2

Time	Effective gradient	$\int_0^{t'} g(t'') dt''$
(0, a)	$-G_0$	$-G_0 \cdot t'$
(a, b)	$-G_0 + g$	$-G_0 \cdot t' + g \cdot (t' - a)$
(b, c)	$-G_0$	$-G_0 \cdot t' + g \cdot (b - a)$
(c, c + a)	$+G_0$	$G_0 \cdot (t' - c) + g \cdot (b - a)$
(c + a, c + b)	$+G_0 - g$	$G_0 \cdot (t' - c) + g \cdot (b - a) - g \cdot (t' - (c + a))$
(c + b, 2c)	$+G_0$	$G_0 \cdot (t' - c)$

Column 3 yields the corresponding time integral of the effective gradient

**Table 1.2** Column 1 is the time parameter with its corresponding time integral of the square of the time integral of the effective gradient in Column 2

Time	$\int_0^t \left( \int_0^{t'} g(t'') dt'' \right)^2$
(0, a)	$\frac{a^3 G_0^2}{3} \text{ or } \frac{\delta_1^3 G_0^2}{3}$
(a, b)	$\frac{-a^3 G_0^2 + ((b-a)(G-g) + aG)^3}{3(G_0-g)} \text{ or } \frac{-\delta_1^3 G_0^2 + (\delta_1(G-g) + \delta_1 G)^3}{3(G_0-g)}$
(b, c)	$\frac{(cG_0 - (b-a)g)^3 - ((b-a)(G-g) + aG)^3}{3G_0} \text{ or } \frac{(\tau G_0 - \delta g)^3 - (\delta(G-g) + \delta_1 G)^3}{3G_0}$
(c, c + a)	$\frac{(cG_0 - (b-a)g)^3 + ((b-a)g - (c-a)G)^3}{3G_0} \text{ or } \frac{(\tau G_0 - \delta g)^3 + (\delta g - (\delta + \delta_2)G)^3}{3G_0}$
(c + a, c + b)	$\frac{((c-b)G_0)^3 + ((b-a)g + (c-a)G)^3}{3(G_0-g)} \text{ or } \frac{(\delta_2 G_0)^3 + (-\delta g + (\delta + \delta_2)G)^3}{3(G_0-g)}$
(c + b, 2c)	$\frac{(c-b)^3 G_0^2}{3} \text{ or } \frac{\delta_2^3 G_0^2}{3}$

The last time integral is either represented with the time parameters a, b, c or the more familiar gradient pulse length  $\delta$ , dead times  $\delta_1$  and  $\delta_2$ , and inter echo spacing  $2\tau$

Finally, all the terms in column 2 are collected, simplified and the result is put into (1.12) to give the attenuation for the simplest PFG NMR sequence

$$I = I_0 e^{-\frac{2\tau}{T_2}} e^{-\gamma^2 g^2 \delta^2 D(\tau - \delta/3) - \gamma^2 G_0^2 D \frac{3}{2} \tau^3 - \frac{\gamma^2 D}{3} (-2\delta_1^3 + 3\delta_1^2 \tau + 3\delta_1 \tau^2 + (\delta_1 + \delta)(2(\delta_1 + \delta)^2 - 3(\delta_1 + \delta)\tau - 3\tau^2)) g \cdot G_0} \quad (1.13)$$

When neglecting the cross terms between the applied and internal magnetic field gradients, the final outcome is the well known PFGSE-attenuation

$$I = I_0 e^{-\frac{2\tau}{T_2}} e^{-\gamma^2 g^2 \delta^2 D(\tau - \delta/3)} \quad (1.14)$$

The observation time is half of the inter echo spacing,  $\tau$ , minus a term that takes into account a finite duration of the gradient pulse,  $\delta/3$ . In Fig. 1.4, the natural logarithm of the attenuation from the spin echo due to incrementing the gradient strength is shown. Knowledge of the time parameters in the pulse sequence and the applied gradient strength used, which in this case goes up to 320 Gauss/cm for the strongest applied gradient, will provide the experimentally determined diffusion coefficient from the slope of the logarithm of the echo attenuation. The slope in this example is linear as the system measured on is bulk water, a single molecular liquid, which should result in a mono exponential decay, and thus a linear slope when taking the logarithm of the attenuation.

Other parameters within the experiment may be varied to achieve an attenuation of the NMR signal, including the inter echo spacing and the gradient pulse length. In bulk or homogeneous systems, where an observation time dependency is not expected on the diffusion coefficient, such an approach method would be

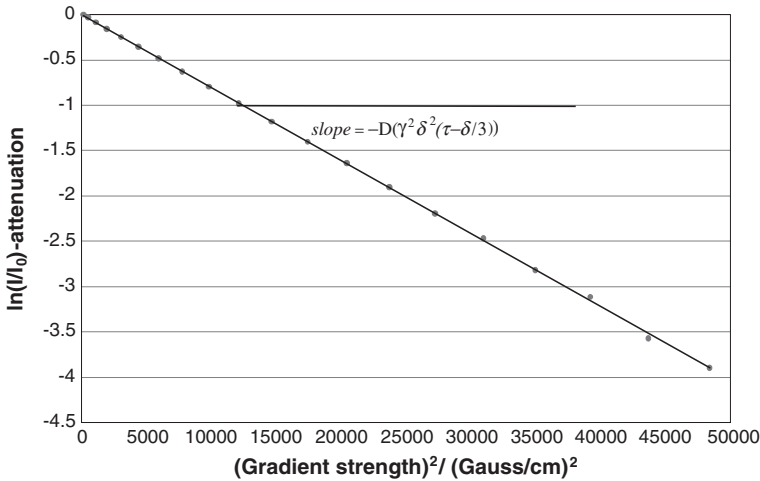


**Fig. 1.4** The logarithm of the echo attenuation as a function of the square of the applied gradient strength



equally applicable. However, once there is any kind of restriction inside the system, be it a solid matrix or a different fluid component, a different apparent diffusion coefficient will be determined by the PFG experiment, which is also dependent on the observation time (gradient pulse separation) and gradient pulse length applied. In these cases, the slope of the logarithm of echo attenuation will no longer be linear. In the case of restricted diffusion studies, alternative sequences are often preferred such as the stimulated echo sequence described in the next section, due to their ability to probe greater length scales.

### 1.3 The Ordinary PFGSTE Sequence

In many systems to be investigated, it is of interest to study the time evolution of the diffusion coefficient. Any spin experiencing restrictions will have their apparent mobility reduced when increasing the observation time, as the likelihood of encountering any obstacle increases as the observation time is increased. As the transverse relaxation time is significantly shorter than the longitudinal relaxation time in many heterogeneous systems, a z-storage delay can be introduced to the PFG sequence as shown in Fig. 1.5, producing the pulsed field gradient

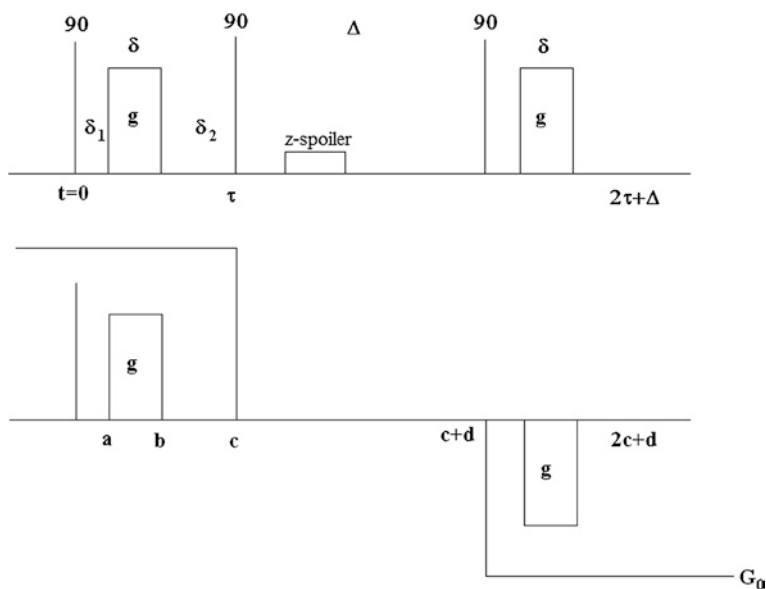


**Fig. 1.5** The pulsed field gradient stimulated echo (PFGSTE) with real (*upper sequence*) and effective (*lower sequence*) gradients. In the  $z$ -storage interval a short spoiler gradient pulse is applied to remove unwanted transverse magnetization coherences. This is known as a spoiler technique and means that during the  $z$ -storage delay any transverse magnetization is subjected to a dephasing gradient pulse

stimulated echo sequence. Here the refocusing  $180^\circ$  RF-pulse is replaced by two  $90^\circ$  RF-pulses separated by a time interval  $\Delta$ . In order to analyze the sequence, as before it is divided into different time intervals and the effective gradients are calculated as for the PFGSE sequence. However, now there is no refocusing RF-pulse that inverts the coupling to the Hamiltonian in the expectation value for the net nuclear magnetization to produce a spin echo. Instead, five echoes are generated in the stimulated echo sequence [34] (see Chap. 3 for further demonstration of the five echoes). As the information on diffusion is apparent in one of the stimulated echoes, the concept of coherence transfer pathways can be applied to follow the magnetization that contributes to the wanted stimulated echo signal. In order to collect this stimulated echo signal only, the phase sequence proposed by Fauth et al. [34], shown in Table 1.3 can be applied.

Following the correct coherence transfer pathway, the effective gradients and corresponding integrals are produced and shown in Table 1.4.

An integration of the square of the expressions in column 3 then provides the expressions that are collected and simplified. The expressions for the echo attenuation from the simplest PFGSTE is then written

$$I = I_0 e^{-\frac{2\tau}{T_2}} e^{-\gamma^2 g^2 \delta^2 D(\Delta + \tau - \delta/3) - \gamma^2 D \frac{\delta}{3} (2\delta_1^2 + 2(\delta_1 + \delta)^2 + \delta_1(2(\delta_1 + \delta) - 3\tau) - 3(\delta_1 + \delta)\tau - 3\tau(\tau + 2\Delta))} \quad (1.15)$$

By neglecting the cross terms the more readable equation is found

$$I = I_0 e^{-\frac{2\tau}{T_2}} e^{-\gamma^2 g^2 \delta^2 D(\Delta + \tau - \delta/3)} \quad (1.16)$$

**Table 1.3** The phase sequence that cancel all echoes except the stimulated echo in the PFGSTE sequence

Sequence #	$\pi/2$ Excitation	Second $\pi/2$	Third $\pi/2$	Receiver
1	+x or 0	+x or 0	+x or 0	−x or $\pi$
2	+x or 0	−x or $\pi$	+x or 0	+x or 0
3	+x or 0	+x or 0	−x or $\pi$	+x or 0
4	+x or 0	−x or $\pi$	−x or $\pi$	−x or $\pi$

**Table 1.4** Column 1 is the time parameter with its corresponding effective gradients in column 2

time	effective gradient	$\int_0^{t'} g(t'') dt''$
(0, a)	$-G_0$	$-G_0 \cdot t'$
(a, b)	$-G_0 + g$	$-G_0 \cdot t' + g \cdot (t' - a)$
(b, c)	$-G_0$	$-G_0 \cdot t' + g \cdot (b - a)$
(c, c + d)	0	$-G_0 \cdot c + g \cdot (b - a)$
(c + d, c + d + a)	$+G_0$	$G_0 \cdot (t' - 2c - d) + g \cdot (b - a)$
(c + d + a, c + d + b)	$+G_0 - g$	$G_0 \cdot (t' - 2c - d) + g \cdot (b - a) - g \cdot (t' - (c + a + d))$
(c + d + b, 2c + d)	$+G_0$	$G_0 \cdot (t' - 2c - d)$

Column 3 yields the corresponding time integral of the effective gradient

Again, the slope of the logarithm of the attenuation as a function of the square of the applied gradient strength will return the diffusion coefficient provided all time parameters and gradient strengths are known. Now, the observation time has an extra term, the z-storage delay  $\Delta$ , which is independent of the gradient pulse length. As the system is affected by  $T_1$ -relaxation during this period, the NMR signal persists longer than if it was subjected to  $T_2$ -relaxation only. Consequently, the observation time dependent diffusion coefficient can be studied up to the order of seconds. Figure 1.6 shows how the time dependency on the diffusion coefficient of water diffusing amongst compact mono sized plastic spheres can be studied. From the initial decay, the short observation times, the surface to volume ratio can be extracted [27], while for the longer observation times the tortuosity limit may be found. The latter is dependent on the NMR signal to persist long enough for the heterogeneity of the sample to be sufficiently probed. In the particular case shown in Fig. 1.6, the spheres have a diameter of 98  $\mu\text{m}$  and then the root of the mean squared displacement assuming bulk diffusion is 150  $\mu\text{m}$  for the longest observation time. Then it can be concluded that the experiment do measure the true tortuosity (Sect. 2.3).

As will be discussed in Chap. 3, there are some major drawbacks using the ordinary PFGSE and PFGSTE sequences. Because of the lack of a refocusing  $180^\circ$  RF pulse within the read and prepare intervals, when the magnetization is subjected to transverse relaxation, it produces a term that couples any background gradient within the sample to the observation time  $\Delta$  (PFGSTE) or  $\tau$  (PFGSE). Thus, the diffusion coefficient measured may be significantly dependent on an uncontrollable parameter, the so-called background gradient strength. The applied gradient strength is controlled by the geometry of the gradient coil and the electrical current being sent through. The background gradient may be an eddy current transient, i.e. varying with time, or simply an internal magnetic field gradient arising from differences in magnetic susceptibility within a

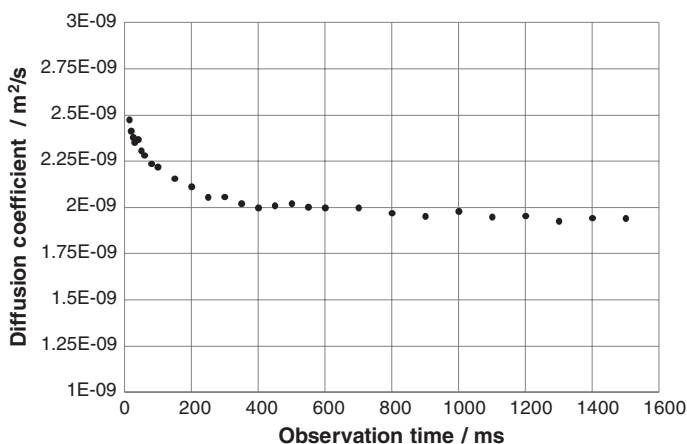


**Fig. 1.6** Diffusion measurements amongst compact mono-sized spheres

heterogeneous sample [35]. The internal gradient may for some systems, such as porous rocks that may contain ferromagnetic impurities, exceed the values of the applied magnetic field gradient. Then the fitted diffusion coefficient from an experiment will be strongly dependent on the porous matrix, and not as much on the true molecular mobility of the fluid confined in the porous system. For many PFG NMR instrumentations (due to eddy current transients) and heterogeneous systems (due to internal magnetic field gradients), it is convenient to have the option of reducing the effect of background gradients, as when applying bipolar gradients in the PFG NMR sequence.

## 1.4 The 11 Interval Bipolar PFGSE

Due to the presence of internal magnetic field gradients, a pulsed field gradient technique that reduces the effect from internal gradients on the echo attenuation as a function of applied gradient strength improves the performance of the PFG NMR sequences. One intuitive approach is to apply such strong gradients that the cross terms that couples the internal and applied gradients are treated as insignificant in comparison [36]. Assuming that the available magnetic field gradient strength is not high enough to employ this technique, more complicated RF-pulse sequences can be employed together with gradients of both polarities in order to minimize the internal gradient effects. In 1973 Blinc et al. [7] proposed a pulsed field gradient sequence which made use of bipolar magnetic field gradients, but this experiment is more complex than the ones proposed by Karlicek et al. [1]. Blinc et al. employed a Waugh-type sequence [7, 21], which significantly reduces the term containing the dipolar interaction in a liquid crystal, together with a Carr Purcell train of  $180^\circ$  RF-pulses [37]. In addition to the removal of the term containing the dipolar interaction, R. Blinc established that their sequence, due to the application of bipolar gradient pulses, also averaged out the coupling to a magnetic field background gradient in the Hamiltonian. Later, Karlicek et al. [1] in 1980 and Cotts et al. [2] in 1989 proposed PFG NMR sequences which by applying bipolar gradient pulses was dedicated specifically to remove the coupling between the applied and internal magnetic field gradients.

The first sequence to be analyzed is the 11 interval bipolar PFGSE sequence [17]. It is the simplest sequence possible that applies bipolar pairs of magnetic field gradients. This sequence minimizes the coupling between the applied and the internal gradients and the observation time is kept at a minimum. It also employs the minimum amount of RF-pulses in the bipolar version of the PFG NMR experiment, from which it follows that signal arising from unwanted coherence transfer pathways will be at a minimum. An RF phase sequence for minimizing the signal arising from unwanted coherence transfer pathways is found in Table 1.5. This phase sequence is constructed specifically for the removal of unwanted coherence transfer pathways as  $P = 0 \rightarrow +1 \rightarrow +1 \rightarrow +1$  and  $P = 0 \rightarrow +1 \rightarrow 0 \rightarrow +1$ , as will be shown in the following (the recipe is found in Appendix). For the first

**Table 1.5** The phase sequence that cancel all echoes except wanted spin echo in the bipolar 11 interval PFGSE sequence

Sequence #	$\pi/2$ Excitation	First $\pi$	Second $\pi$	Receiver
1	+x or 0	+y or $\pi/2$	-y or $3\pi/2$	+x or 0
2	+x or 0	+y or $\pi/2$	+y or $\pi/2$	+x or 0
3	+x or 0	+y or $\pi/2$	-x or $\pi$	-x or $\pi$
4	+x or 0	-x or $\pi$	+y or $\pi/2$	-x or $\pi$

coherence transfer pathway,  $\Delta P_1$  is +1 at the point of application of the first RF-pulse, then  $\Delta P_{2,3}$  is zero for the rest of the pathway. Thus the resulting phase  $\varphi$  is 0 for all pathways, and as the receiver phase is 0, 0,  $\pi$ , and  $\pi$ , the signal from this pathway will be cancelled.

For the second pathway the calculation for the resulting phase for the 4 different phase sequences shown in Table 1.5 is

$$\varphi = \sum_{j=1}^3 \Delta P_j \varphi_j = \begin{bmatrix} +1 \cdot 0 - 1 \cdot \pi/2 + 1 \cdot 3\pi/2 = \pi \\ +1 \cdot 0 - 1 \cdot \pi/2 + 1 \cdot \pi/2 = 0 \\ +1 \cdot 0 - 1 \cdot \pi/2 + 1 \cdot \pi = \pi/2 \\ +1 \cdot 0 - 1 \cdot \pi + 1 \cdot \pi/2 = -\pi/2 \end{bmatrix}, \quad \varphi_{RECEIVER} = \begin{bmatrix} 0 \\ 0 \\ \pi \\ \pi \end{bmatrix}$$

Thus the contribution from the pathway  $P = 0 \rightarrow +1 \rightarrow 0 \rightarrow +1$  will also be cancelled. In addition unwanted coherence transfer pathways as  $P = 0 \rightarrow -1 \rightarrow +1 \rightarrow +1$  will not contribute to the NMR echo signal as the sequence of effective gradient pulses does not result in a gradient echo (Fig. 1.7).

The effective gradients and corresponding integrals are as shown in Table 1.6.

The resulting equation from the calculation is

$$I = I_0 e^{-\frac{4\tau}{T_2}} e^{-\gamma^2 f^2 \delta^2 D(\tau - \delta/3) - \gamma^2 g^2 \delta^2 D(3\tau - \delta/3) - 2\gamma^2 f g \delta^2 D(\tau) - \gamma^2 D \delta (\delta_1 - \delta_2)(\tau)(g+f)G_0 - \frac{4\tau^3 G_0}{3}} \quad (1.17)$$

Denoting  $g = g_{cal}(i)$  and  $f = g_{cal}(i - x)$ , where  $g_{cal}$  is the gradient strength per arbitrary unit, and (i) and (i - x) are gradient amplitudes in arbitrary units, the equation is simplified to

$$I = I_0 e^{-\frac{4\tau}{T_2}} e^{-\gamma^2 g^2 (2\delta)^2 D\left[\frac{3\tau}{2} - \delta/6\right] \left[i - \frac{x}{2} \left(\frac{\tau - \delta/6}{\frac{3}{2}\tau - \delta/6}\right)\right]^2 - \gamma^2 D(2i-x)\delta(\delta_1 - \delta_2)(\tau)g_{cal}G_0 - \frac{4\tau^3 G_0}{3} + offset} \quad (1.18)$$

x provides the difference in applied gradient strength, and the offset is a small constant term due to this difference in amplitude of f and g, and is given by

$$offset = -\gamma^2 \delta^2 D \left[ \frac{(\tau - \delta/6)^2}{\frac{3}{2}\tau - \delta/6} - (\tau - \delta/3) \right] x^2 \quad (1.19)$$

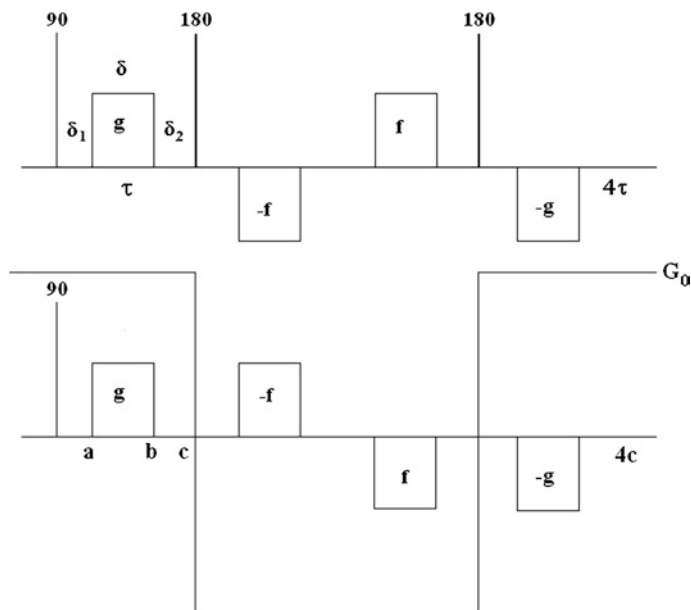


**Fig. 1.7** The 11 interval bipolar PFGSE sequence with real (*upper sequence*) and effective gradients (*lower sequence*)

**Table 1.6** Column 1 is the time parameter with its corresponding effective gradients in column 2

Time	Effective gradient	$\int_0^{t'} g(t'') dt''$
(0, a)	$+G_0$	$+G_0 \cdot t'$
(a, b)	$+G_0 + g$	$+G_0 \cdot t' + g \cdot (t' - a)$
(b, c)	$+G_0$	$+G_0 \cdot t' + g \cdot (b - a)$
(c, c + a)	$-G_0$	$-G_0 \cdot (t' - 2c) + g \cdot (b - a)$
(c + a, c + b)	$-G_0 + f$	$-G_0 \cdot (t' - 2c) + f \cdot (t' - (c + a)) + g \cdot (b - a)$
(c + b, 2c)	$-G_0$	$-G_0 \cdot (t' - 2c) + f \cdot (b - (c + a)) + g \cdot (b - a)$
(2c, 2c + a)	$-G_0$	$-G_0 \cdot (t' - 2c) + f \cdot (b - a) + g \cdot (b - a)$
(2c + a, 2c + b)	$-G_0 - f$	$-G_0 \cdot (t' - 2c) - f \cdot (t' - (2c + a)) + f \cdot (b - a) + g \cdot (b - a)$
(2c + b, 3c)	$-G_0$	$-G_0 \cdot (t' - 2c) + g \cdot (b - a)$
(3c, 3c + a)	$+G_0$	$+G_0 \cdot (t' - 4c) + g \cdot (b - a)$
(3c + a, 3c + b)	$+G_0 - g$	$+G_0 \cdot (t' - 4c) - g \cdot (t' - (3c + a)) + g \cdot (b - a)$
(3c + b, 4c)	$+G_0$	$+G_0 \cdot (t' - 4c)$

Column 3 yields the corresponding time integral of the effective gradient

When  $x = 0$  there is no difference in amplitudes of  $f$  and  $g$ , and the offset term equals 0. Equations (1.17–1.19) are valid regardless of whether equal or unequal bipolar gradients are being used. A small cross term exists between the applied and the internal magnetic field gradient. This term is canceled provided

$\delta_1 = \delta_2$ . It follows from the evaluation of the echo attenuation that the application of bipolar magnetic field gradients significantly reduces or cancels the cross term between the applied and the internal magnetic field gradients. But is there an intuitive explanation to this? Such an explanation can be arrived at by examination of the effective gradients in Table 1.1 for the ordinary PFGSE. It can be seen that the effective applied gradient changes polarity when the background gradient changes polarity. This is a consequence of the  $180^\circ$  RF pulse on the Hamiltonian (Appendix). As the square of the effective gradients generates cross terms between the applied and background gradients in both the prepare and read intervals, these terms will have the same polarity and will not cancel out. If the read and prepare intervals are extended by adding  $180^\circ$  RF-pulses in the PFGSE sequence and applying bipolar gradients in the prepare and read intervals, there will be two cross terms generated between the applied and background gradients in both intervals, but with opposite polarity (see Table 1.6). These cross terms are cancelled before taking the square of the effective gradients, leaving the square of the applied gradient and the square of the background gradient. As the latter is constant, the applied gradient strength may be incremented and the term containing the background gradient can be treated as an offset term.

## 1.5 The 13 Interval Bipolar PFGSTE

Even though the 11-interval sequence is the simplest and most effective in canceling out the impact from internal magnetic field gradients in the PFG-NMR experiment, there is often a need for measuring the diffusion coefficient as a function of observation time. To do so, it is again convenient to proceed to the stimulated echo sequence where there is access to a z-storage delay, which can be used for the study of observation time dependent diffusivity. The 13 interval bipolar PFGSTE sequence, shown in Fig. 1.8, is a stimulated echo sequence but with refocussing  $180^\circ$  RF pulses in the prepare and read intervals [2, 5]. On each side of the  $180^\circ$  RF pulse, applied pulsed gradients of different polarity and different strength,  $f$  and  $g$ , are placed.

The appropriate phase sequence is found in Table 1.7. When using unequal bipolar gradients  $g$  and  $f$  it is sufficient to use the first four (#1–#4), as the unequal pairs cancel out the pathway  $p \rightarrow 0 \rightarrow +1 \rightarrow +1$  in the read interval. The second part of the phase sequence must be included if equal bipolar gradients are applied ( $g = f$ ). This phase sequence was developed by Wu et al. [38] and is designed to cancel the coherence transfer pathway  $p \rightarrow 0 \rightarrow +1 \rightarrow +1$  from the read interval of the pulse sequence.

Following the correct coherence transfer pathway, the effective gradients and corresponding integrals are found as shown in Table 1.8.

The resulting equation from the calculation is

$$I = I_0 e^{-\frac{4\tau}{T_2}} e^{-\gamma^2 f^2 \delta^2 D(\Delta + \tau - \delta/3) - \gamma^2 g^2 \delta^2 D(\Delta + 3\tau - \delta/3) - 2\gamma^2 f g \delta^2 D(\Delta + \tau) - \gamma^2 D \delta (\delta_1 - \delta_2)(\tau)(g+f) G_0 - \frac{4\tau^3 G_0}{3}} \quad (1.20)$$

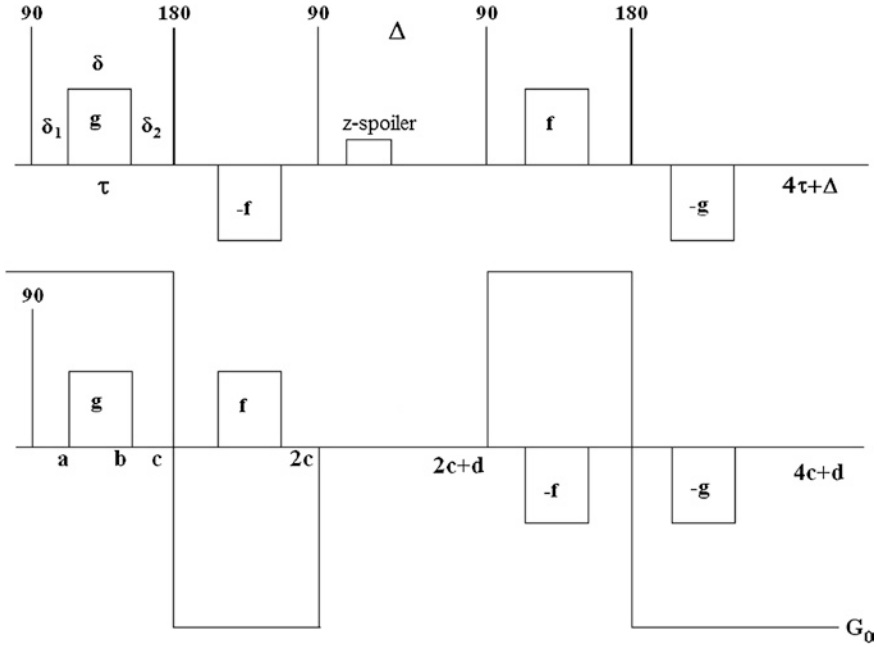


**Fig. 1.8** The 13 interval bipolar PFGSTE sequence with real (*upper sequence*) and effective (*lower sequence*) gradients. In the z-storage interval a short spoiler gradient pulse is applied to spoil unwanted signal

**Table 1.7** The phase sequences that cancel all echoes except wanted stimulated echo in the bipolar 13 interval PFGSTE sequence

Sequence #	$\pi/2$ Excitation	Second $\pi/2$	Third $\pi/2$	Receiver
1	+x or 0	+x or 0	+x or 0	-x or $\pi$
2	+x or 0	-x or $\pi$	+x or 0	+x or 0
3	+x or 0	+x or 0	-x or $\pi$	+x or 0
4	+x or 0	-x or $\pi$	-x or $\pi$	-x or $\pi$
5	+x or 0	+x or 0	+y or $\pi/2$	+y or $\pi/2$
6	+x or 0	-x or $\pi$	+y or $\pi/2$	-y or $3\pi/2$
7	+x or 0	+x or 0	-y or $3\pi/2$	-y or $3\pi/2$
8	+x or 0	-x or $\pi$	-y or $3\pi/2$	+y or $\pi/2$

Denoting  $g = g_{cal}(i)$  and  $f = g_{cal}(i - x)$ , where  $g_{cal}$  is the calibrated gradient strength per arbitrary unit, and  $(i)$  and  $(i - x)$  are the gradient amplitudes in arbitrary units, the equation is simplified to

$$I = I_0 e^{-\frac{4\tau}{T_2}} e^{-\gamma^2 g^2 (2\delta)^2 D \left[ \Delta + \frac{3\tau}{2} - \delta/6 \right] \left[ i - \frac{x}{2} \left( \frac{\Delta + \tau - \delta/6}{\Delta + \frac{3}{2}\tau - \delta/6} \right) \right]^2 - \gamma^2 D (2i - x) \delta (\delta_1 - \delta_2) (\tau) g_{cal} G_0 - \frac{4\tau^3 G_0}{3} + offset} \quad (1.21)$$



**Table 1.8** Column 1 is the time parameter with its corresponding effective gradients in column 2

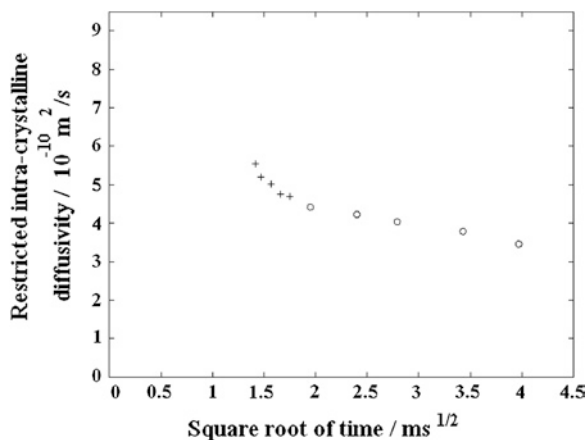
Time	Effective gradient	$\int_0^{t'} g(t'') dt''$
(0, a)	$+G_0$	$+G_0 \cdot t'$
(a, b)	$+G_0 + g$	$+G_0 \cdot t' + g \cdot (t' - a)$
(b, c)	$+G_0$	$+G_0 \cdot t' + g \cdot (b - a)$
(c, c + a)	$-G_0$	$-G_0 \cdot (t' - 2c) + g \cdot (b - a)$
(c + a, c + b)	$-G_0 + f$	$-G_0 \cdot (t' - 2c) + f \cdot (t' - (c + a)) + g \cdot (b - a)$
(c + b, 2c)	$-G_0$	$-G_0 \cdot (t' - 2c) + f \cdot (b - (c + a)) + g \cdot (b - a)$
(2c, 2c + d)	0	$f \cdot (b - a) + g \cdot (b - a)$
(2c + d, 2c + d + a)	$+G_0$	$+G_0 \cdot (t' - 2c + d) + f \cdot (b - a) + g \cdot (b - a)$
(2c + d + a, 2c + d + b)	$+G_0 - f$	$+G_0 \cdot (t' - 2c + d) - f \cdot (t' - (2c + d + a)) + f \cdot (b - a) + g \cdot (b - a)$
(2c + d + b, 3c + d)	$+G_0$	$+G_0 \cdot (t' - 2c + d) + g \cdot (b - a)$
(3c + d, 3c + d + a)	$-G_0$	$-G_0 \cdot (t' - 4c + d) + g \cdot (b - a)$
(3c + d + a, 3c + d + b)	$-G_0 - g$	$-G_0 \cdot (t' - 4c + d) - g \cdot (t' - (3c + a)) + g \cdot (b - a)$
(3c + d + b, 4c + d)	$-G_0$	$-G_0 \cdot (t' - 4c + d)$

Column 3 yields the corresponding time integral of the effective gradient

x provides the difference in applied gradient strength, and the offset is a small constant term due to this difference in amplitude of f and g.

In work with observation time dependent apparent diffusion measurements it may be of interest to measure the initial slope of the time dependent diffusion coefficient, to produce the surface to volume ratio independent of surface relaxivity [27]. Due to the finite duration of the z-storage delay, there is a limit to how short the observation time can be for the 13 interval PFGSTE sequence. It may therefore be convenient to combine the 11 interval PFGSE and the 13 interval PFGSTE as shown in Fig. 1.9. Here a combination of the two sequences is shown, and it is quite evident that new information is gathered by adding the data points at the shortest observation times acquired with the 11 interval PFGSE [17].

**Fig. 1.9** The observation time dependent intra-crystallite diffusivity of ethane in H-ZSM5. “+”, data acquired with the 11 interval PFGSE sequence; and “O”, data acquired with the 13 interval PFGSTE sequence



## 1.6 The Convection Compensated PFG NMR Sequences

When performing diffusion experiments in solutions or in low viscosity systems, it is important to have a homogeneous heating of the sample and an accurate temperature control of the system. Otherwise, flow effects due to convection currents will disrupt the diffusion measurement. In addition, the effects of convection can be minimized by the use of so-called convection compensated PFG NMR sequences that serve to suppress effects caused by convection/laminar flow. It can be shown [8] that the consequence of convection within the sample on the expectation value for the magnetization from an arbitrary pulsed field gradient sequence in the presence of a velocity term,  $v$ , is

$$M^+ = M_0^+ e^{-\frac{t_1}{T_2}} e^{-\frac{t_2}{T_1}} e^{-\gamma^2 D \int_0^t (\int_0^{t'} g(t'') dt'')^2 dt'} e^{i v \gamma \int_0^t (\int_0^{t'} g(t'') dt'') dt'} \quad (1.22)$$

Already in 1954 Carr and Purcell [39] noted that even echoes in a multi spin-echo experiment (CPMG train) [37] were convection compensated. Thus, when assuming a constant velocity term experienced by the diffusing molecules, a double pulsed field gradient spin or stimulated echo sequence would suppress the effect from convection in the diffusion experiment. In principle, monopolar pulsed field gradient experiments (two times the ordinary PFGSE or PFGSTE) could be used, but this leads to substantial eddy current transients that would lead to increased line width and baseline distortions in high resolution Fourier transformed spectra. In order to simultaneously compensate for convection and simultaneously minimize the effect from eddy current transients, instead double versions of the 11 interval bipolar PFGSE or 13 interval bipolar PFGSTE [8] can be used. However, one major drawback using the double bipolar version is the lengthened duration of the sequence. If the molecules undergo fast transverse relaxation, the achievable to signal to noise ratio may become an issue. Another challenge might be the number of scans required to perform a proper phase sequence to eliminate signal from unwanted coherence transfer pathways [8]. This number could be much larger than what is required for a system to achieve a satisfactorily signal to noise ratio in the echo signal. This would unnecessarily extend the experiment time.

Realizing that the bipolar gradient pairs are not required for suppressing the coupling between applied and internal magnetic field gradients in liquid systems, the gradients of opposite polarity are placed as shown in Fig. 1.10 for the ordinary

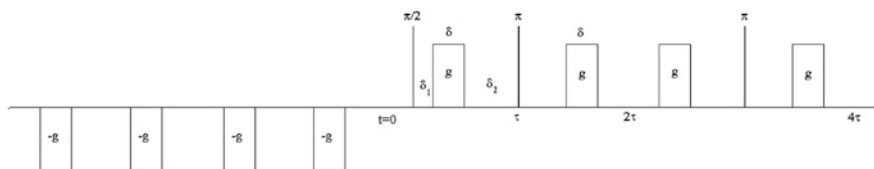


**Fig. 1.10** A double PFGSE with preparatory gradients of opposite polarity

double PFGSE sequence [40]. Here the gradient pulses of opposite polarity are placed before the  $90^\circ$  RF excitation pulse, in order to reduce the eddy current transients following the PFGSE sequence. Conclusively, the eddy current transients will be greatly reduced while the double spin echo will be the simplest possible for achieving convection compensation. The echo attenuation for the sequence is written

$$I = I_0 e^{-\frac{2\tau}{T_2}} e^{-2\gamma^2 g^2 \delta^2 D(\tau - \delta/3)} \quad (1.23)$$

If it is crucial to include a storage period of the NMR signal between motional encoding and decoding, for example in order to have a proper attenuation of a slowly moving macro molecule in a solution, a double version of the pulsed field gradient stimulated echo sequence should be employed. The gradient pulses of opposite polarity should be placed as shown in Fig. 1.11. This arrangement allows the shortest duration between the bipolar pairs. Thus, the first gradient of opposite polarity is placed early in the first z-storage interval to compensate for the eddy current transients arising from first applied gradient pulse. In order to optimize the positioning of the preparatory gradients on high field systems, the spin lock signal can be monitored (if available). The lock signal is very sensitive to eddy current transients, and Fig. 1.12 shows how the application of preparatory gradient pulses

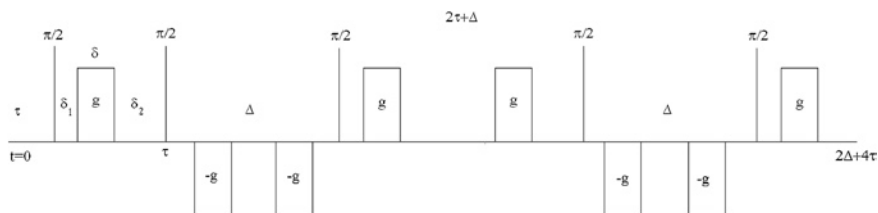


**Fig. 1.11** A double PFGSTE with preparatory gradients of opposite polarity

**Fig. 1.12** Recording of the lock deuterium signal during a mono-polar double PFGSTE sequence (*dashed line*) and the double PFGSTE with preparatory gradient pulses (*solid line*) [40]

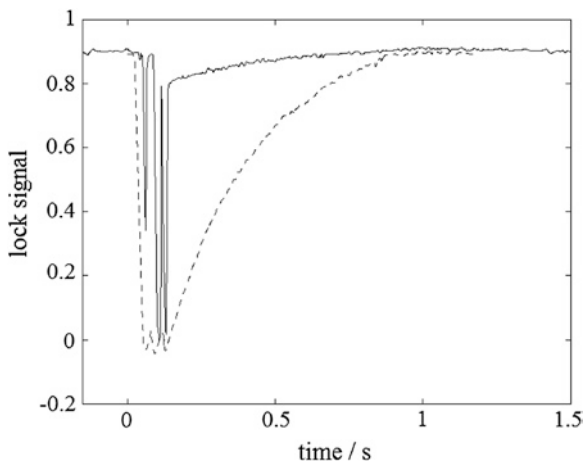
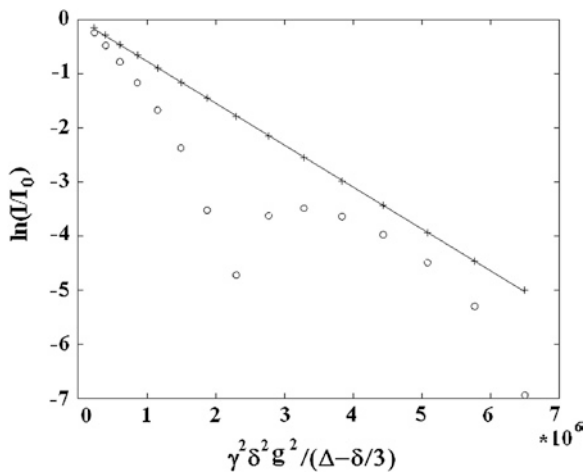


**Fig. 1.13** Comparing the diffusion with (“+”) or without (“O”) convection compensation, using the double PFGSE sequence on acetonitrile at 15 °C [40]



significantly reduces the strength of eddy current transients after having optimized their positions. The impact of this reduction in eddy current field, is that both the phase and baseline error in the Fourier-transformed spectra are significantly reduced [40].

$$I = I_0 e^{-\frac{2\tau}{T_2}} e^{-2\gamma^2 g^2 \delta^2 D(\Delta + \tau - \delta/3)} \quad (1.24)$$

In Fig. 1.13, the effect of introducing a double pulsed field gradient spin echo sequence as compared to a single pulsed field gradient spin echo sequence in the presence of convection can be seen. The system studied was a solution of acetonitrile at 15 °C [6]. While the double version produces a linear decay of the logarithm of the echo attenuation as a function of the square of the applied gradient strength, the single spin echo approach yields a non-linear decay due to a non-zero convection term.

## 1.7 The Spoiler Recover Pulse Sequence

A long acquisition time may be an important limiting factor when performing a PFG NMR experiment. Samples, being biological tissues, emulsions or brine saturated rock core plugs, may not be stable for as long as the conventional PFG NMR experiment lasts. In conventional diffusion and two-dimensional experiments, it is usual to wait 5 times the longitudinal relaxation time between each scan in order to ensure that the system returns to its equilibrium state. Consequently, a 2-dimensional  $T_1$ - $T_2$  experiment may last for several hours depending on the number of scans and variable z-storage delays. Under these conditions, biological tissue may start to deteriorate, emulsions may start to separate, or the brine from the core plug may evaporate during the experiment, consequently leading to unstable conditions and unreliable results. In addition, in dynamic systems instability is often a key

factor to be studied, such as the study of separation processes in water in oil emulsions by adding a demulsifier. This separation process may take from seconds up to days, depending on the experimental settings on the system under investigation (see Chap. 7). A PFG NMR method that bypassed the required 5 times  $T_1$  between the scans while maintaining quantitative diffusion information enhances the range of systems that PFG NMR can be used to study. This requirement initiated the development of the spoiler recovery sequence at low resolution conditions (0.05 T permanent magnet) [41]. The development of the spoiler recovery sequence makes it possible to perform rapid measurements of diffusion characteristics and  $T_2$  relaxation. In emulsion characterization that would implicate a possibility of measuring droplet size distribution and/or S/V profiles on unstable emulsions which have instability on a short timescale [42]. Further investigations established that the method can also be used at much higher field, where the effect from radiation damping [43] (Chap. 6) may complicate the diffusion measurements. Using the spoiler recovery approach radiation damping artefacts were removed at 11.7 T as well as the need for a delay of 5 times  $T_1$  between the scans [44].

A common technique used in order to reduce the measurement time of experiments is the option of small flip angles for the initial  $90^\circ$  RF-pulse and/or RF-trains to saturate the artefacts arising from short wait time between the scans, but this approach is not well suited for low resolution NMR [45–47]. The reduction in signal intensity requires more scans to be accumulated, and thus increases the measurement time. Instead, a sequence that produces a situation where the net nuclear magnetic moment of the nuclear spins is zero as an outcome is a preferred solution, i.e. launching the spoiler recovery sequence as shown in Fig. 1.14. The first  $90^\circ$  RF-pulse flips the magnetization initially along the z-direction into the transverse (xy) plane where it is subjected to a relatively long gradient pulse of enough strength to change the phase of the spins by a relatively large value. After the application of the first gradient pulse, GS1, the net nuclear magnetization is zero and the nuclear spin vectors have dephased to cover the whole xy-plane. Then another  $90^\circ$  RF-pulse is applied to rotate the plane of nuclear spin vectors to a plane transverse to the xy-plane, followed by a new gradient pulse of opposite polarity to the first one and with a different gradient strength and duration. The

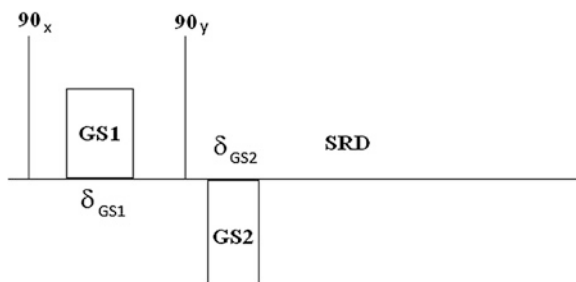


**Fig. 1.14** The spoiler recovery sequence, applies two  $90^\circ$  RF-pulses and a bipolar pair of gradients of different duration and strength. Then a spoiler recovery delay (SRD) is set up for recovery of magnetization along the direction of the external field

idea is then to make the nuclear spin vectors to dephase uniformly in space, where again the net nuclear magnetization is zero after the application of the second gradient pulse.

The basic requirement for avoiding gradient echoes after the application of the second gradient pulse is the following relation

$$\gamma \text{GS1} \int_0^{\delta_{\text{GS1}}} z_1(t) dt \neq \gamma \text{GS2} \int_0^{\delta_{\text{GS2}}} z_2(t) dt \quad (1.25)$$

$\delta_{\text{G1}}$  and  $\delta_{\text{G2}}$  are the durations of the spoiler gradient pulses,  $Z_{1,2}(t)$  are the molecular positions at the time of the two gradient pulses, and  $\gamma$  is the gyromagnetic ratio. Then the following 3 coherence transfer pathways are not refocused,  $p \rightarrow 0 \rightarrow 1 \rightarrow 1$ ,  $p \rightarrow 0 \rightarrow -1 \rightarrow 1$ , and  $p \rightarrow 0 \rightarrow 0 \rightarrow 1$ . To acquire noise only during the spoiler recovery delay (SRD) it is therefore important to choose the GS1 and GS2 values as a bipolar pair of different duration and strength and in accordance with (1.25). As will be shown in Chap. 6, the spoiler recovery approach applies equally well at an external magnetic field of 0.05 T as well as 14.1 T. With the introduction of the spoiler recovery (SR) sequence, two-dimensional acquisition schemes such as a two-dimensional  $T_1$ - $T_2$  experiment become more practical. These experiments will be introduced in the next section.

## 1.8 Combined Two Dimensional Diffusion, $T_1$ and/or $T_2$ Pulse Sequences

In the following section, the pulse sequence/experiment and its corresponding attenuation for a homogeneous system will be provided for three different two-dimensional PFG NMR experiments. These will serve as examples of sequences that may be constructed from the basic one-dimensional PFG NMR experiments, as there are numerous variants that can be constructed, some of which are presented in Chap. 6.

Figure 1.15 shows the combined SR-11-interval PFGSE-CPMG sequence. While fixing the spoiler recovery delay to a constant value, the applied gradient

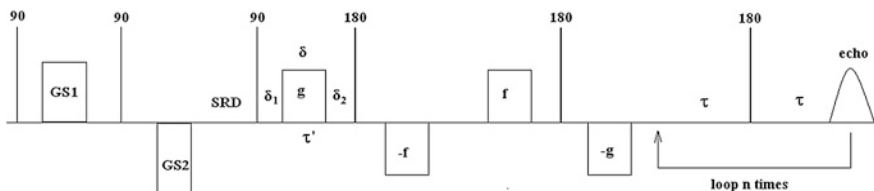


**Fig. 1.15** The combined SR-Diffusion- $T_2$  experiment

strength may be incremented and a CPMG-echo train as a function of applied gradient strength can be recorded. The echo attenuation for this sequence is written as follows

$$I = I_0 \sum_n e^{-\frac{4\tau'}{T_2} - \gamma^2 g^2 (2\delta)^2 D \left[ \Delta + \frac{3\tau'}{2} - \delta/6 \right] \left[ i - \frac{\gamma}{2} \left( \frac{\Delta + \tau' - \delta/6}{\Delta + \frac{3}{2}\tau' - \delta/6} \right) \right]^2} e^{-\frac{2n\tau}{T_2}} \quad (1.26)$$

The experiment illustrated in Fig. 1.15 is referred to as a Diffusion-T<sub>2</sub> experiment.

Figure 1.16 shows a combined SR-11-interval PFGSE sequence. For different durations of SRD the applied pulsed field gradient strength is incremented. The attenuation for this sequence is written as follows

$$I = I_0 (1 - e^{-\frac{SRD}{T_1}}) e^{-\frac{4\tau'}{T_2} - \gamma^2 g^2 (2\delta)^2 D \left[ \Delta + \frac{3\tau'}{2} - \delta/6 \right] \left[ i - \frac{\gamma}{2} \left( \frac{\Delta + \tau' - \delta/6}{\Delta + \frac{3}{2}\tau' - \delta/6} \right) \right]^2} \quad (1.27)$$

The experiment illustrated in Fig. 1.16 is referred to as a Diffusion-T<sub>1</sub> experiment, i.e. a diffusion experiment is conducted for a set of SRD's.

Figure 1.17 shows the combined SR - CPMG sequence. By varying the SRD a CPMG-train may be recorded as a function of the SRD. The attenuation for this sequence is written as follows

$$I = I_0 (1 - e^{-\frac{SRD}{T_1}}) \sum_n e^{-\frac{2n\tau}{T_2}} \quad (1.28)$$

The experiment illustrated in Fig. 1.17 is referred to as a T<sub>1</sub>-T<sub>2</sub> experiment.

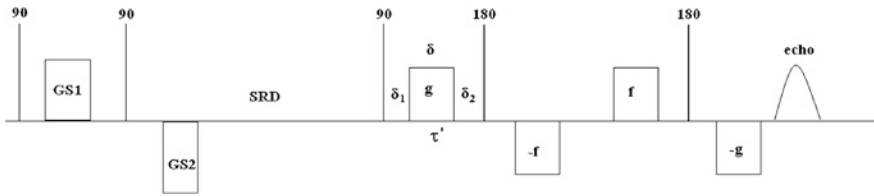


Fig. 1.16 The combined SR-Diffusion-T<sub>1</sub> experiment

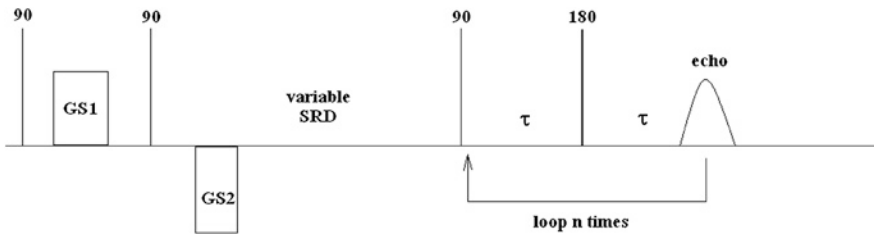


Fig. 1.17 The combined SR-T<sub>1</sub>-T<sub>2</sub> experiment

There are numerous other variations of the two-dimensional experiments, but the experiments presented here are the basic ones that apply the spoiler recovery sequence to measure  $T_1$ ,  $T_2$  and/or Diffusion, and to minimize the experimental time. These sequences or variations of them are exploited in a number of applications which are presented in Chaps. 6–9.

## Appendix

### *The Expectation Value for the Net Nuclear Magnetization in the PFGSE*

The concept of a density matrix is convenient when working with practically non-interacting spins, as is the case for particles in motion. However, there is a requirement to calculate the magnetization that is detectable from an NMR pulse sequence containing RF-pulses and magnetic field gradient pulses. A differential equation reflecting the spin dynamics of the system must be found and solved. The solution of the equation will be dependent on the interaction between the spin system and the time dependent external field  $\vec{H}(t)$ , and will provide information on the evolution of the spin system when being subjected to RF pulses and magnetic field gradients. The derivation below is motivated by the need for a way to calculate the magnetization that is detectable from an NMR pulse sequence containing RF-pulses and magnetic field gradient pulses.

Assuming that the probability function of an ensemble of spins is the sum of a set of orthogonal eigen functions, it can be written as follows [21]

$$\psi = \sum_n c_n U_n \quad (1.29)$$

Here  $c_n$  is the time dependent part while  $U_n$  is the time independent part. The expectation value for the magnetization of the ensemble then is

$$\langle M_x \rangle = \sum_{m,n} c_m^* c_n \langle m | M_x | n \rangle = \sum_{m,n} \langle n | P | m \rangle \langle m | M_x | n \rangle = \sum_n \langle n | P M_x | n \rangle = \text{Tr}\{P M_x\} \quad (1.30)$$

where  $P$  is defined as  $\langle n | P | m \rangle = c_n c_m^*$ . When looking at the ensemble average, the average over all possible time dependent wave functions  $c_n$ , the definition of the density matrix  $\rho_d$  may be produced.

$$\langle n | \rho_d | m \rangle = \overline{\langle n | P | m \rangle} = \overline{c_n c_m^*} \quad (1.31)$$

The average expectation value of the magnetization of the spin ensemble is then written

$$\overline{\langle M_x \rangle} = \text{Tr}\{\rho_d M_x\} \quad (1.32)$$

The physical interpretation of  $\rho_d$  becomes apparent when considering  $\langle n | \rho_d | n \rangle = \overline{c_n c_n^*}$ . This is the probability of finding the system in state  $n$ , and



therefore the trace of  $\rho M_x$  ( $Tr\{\rho M_x\}$ ) is the sum of the expectation values for the magnetization of all states, each multiplied by the probability of finding that state occupied. Now consider the Schrödinger equation

$$-\frac{\hbar}{i} \frac{\partial \psi}{\partial t} = \mathbf{H} \psi \quad (1.33)$$

Expanding  $\psi$  in the orthogonal set of eigen functions, and multiplying it with one of the functions  $c_k|k\rangle$ , and perform a volume integration one finds [21]

$$-\frac{\hbar}{i} \frac{\partial c_k}{\partial t} = \sum_n c_n \langle k | \mathbf{H} | n \rangle \quad (1.34)$$

Regarding the ensemble average a differential equation for the density matrix  $\rho_d$  can now be found as

$$\frac{\partial \rho_d}{\partial t} = \frac{\partial}{\partial t} (c_k c_m^*) = c_k \frac{\partial c_m^*}{\partial t} + \frac{\partial c_k}{\partial t} c_m^* = \frac{i}{\hbar} [\rho_d, \mathbf{H}] \quad (1.35)$$

In the rotating frame of reference, the solution for a time independent Hamiltonian can be written [21]

$$\rho_R(t) = e^{-\frac{i}{\hbar} \mathbf{H}_{\text{eff}} t} \rho_R(0) e^{\frac{i}{\hbar} \mathbf{H}_{\text{eff}} t} \quad (1.36)$$

where  $\mathbf{H}_{\text{eff}} = -\hbar(\gamma H_0 - \omega) I_z \hat{k} - \gamma \hbar H_1(t) I_x \hat{i}$ , and  $\rho_R = e^{-i\omega t I_z} \rho_d e^{i\omega t I_z}$ . This is the starting point when evaluating the influence of the magnetic field from an RF-coil has on the evolution of the magnetization of the nuclear spins. Before evaluating this influence, knowledge on the density matrix at thermal equilibrium must be obtained. For the system of non-interacting spins,  $\rho_R(0)$  is given by

$$\rho_R(0) = \frac{1}{Z} e^{-\gamma \hbar H_0 I_z / kT} \quad (1.37)$$

$Z$  is the partition function,  $k$  is the Boltzmann constant and  $T$  is the absolute temperature [21]

### ***The Response to a 90° RF-Pulse***

In the previous section the way of achieving the expectation value for the net nuclear magnetization was outlined, and now this can be used to evaluate the effect of applying a rotating  $H_1$ -field with frequency  $\omega = \gamma H_0$  in the x-direction of the rotating frame of reference at  $t = 0$ , and with a duration  $t_1$  such that  $\gamma H_1 t_1 = \frac{\pi}{2}$ . In this situation  $\rho_R(t_1)$  is written [21]

$$\rho_R(t_1) = e^{\frac{i}{\hbar} \frac{\pi}{2} I_x} \rho_R(0) e^{-\frac{i}{\hbar} \frac{\pi}{2} I_x} = e^{\frac{i}{\hbar} \frac{\pi}{2} I_x} \frac{e^{-\gamma \hbar H_0 I_z / kT}}{Z} e^{-\frac{i}{\hbar} \frac{\pi}{2} I_x} \quad (1.38)$$

Employing the high temperature approximation for the partition function

$$\rho_R(0) = \frac{1}{(2I + 1)} \left(1 - \frac{\gamma \hbar H_0}{kT} I_z\right) \quad (1.39)$$

Expanding the other exponentials in (1.38) and using the commutation relations, cyclic permutations from  $[I_x, I_y] = I_x I_y - I_y I_x = iI_z$ , it can be shown that the expectation value for the magnetization in the y-direction of the rotating frame of reference can be written [21]

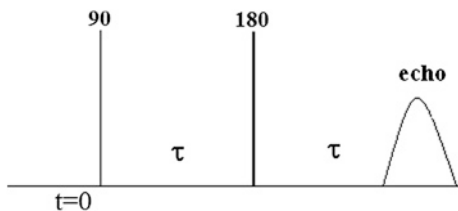
$$\langle M_y(t_1) \rangle = \gamma \hbar \text{Tr} \{ \rho_R(t_1) I_y \} = \frac{\gamma^2 \hbar^2 H_0}{(2I + 1)kT} \text{Tr} \{ I_y^2 \} = \gamma^2 \hbar^2 H_0 \frac{NI(I + 1)}{3kT} \quad (1.40)$$

### *The Response to a Spin Echo Experiment*

The pulse sequence for a spin echo experiment is shown in Fig. 1.18. At  $t = 0$  the net magnetization is in the z-direction. After applying the first  $90^\circ$  RF-pulse,  $\gamma H_1 t_1 = \frac{\pi}{2}$ , the magnetization has been flipped to be aligned with the negative y-axis in the rotating frame of reference. At  $t_2$  the second RF-pulse is applied,  $\gamma H_1 (t_3 - t_2) = \pi$ , and depending on the direction of this  $180^\circ$  RF pulse, the nuclear spins will be flipped  $180^\circ$  around the negative y-axis or flipped  $180^\circ$  to be aligned with the positive direction of the y-axis. In the following, a  $180^\circ$  RF-pulse in the same direction as the  $90^\circ$  pulse will be assumed (i.e.  $H_1$  along the x-axis in the rotating frame of reference). Now the evolution of the magnetization after the application of the second RF-pulse can be evaluated. In order to do this an expression for the density matrix at  $t > t_3$  needs to be found, and this can be used to calculate the expectation value for the magnetization given by (1.32). In the rotating frame of reference, the Hamiltonian is independent of time except when switching on and off the RF magnetic field. Even if there is a discontinuity of the Hamiltonian at  $t = 0, t_1, t_2$  and  $t_3$ , the density matrix, which reflects the probability density of spins, must be continuous. This can be shown by integrating over the discontinuities letting the limits approach the time of the discontinuity [21]. The solution of the density matrix subjected to the spin echo pulse sequence can therefore be done stepwise, and at  $t = 0^-$  thermal equilibrium may be assumed. The density matrix is then given by the Boltzmann factor

$$\rho_R(0^-) = \frac{e^{-\gamma \hbar H_0 I_z / kT}}{Z} \quad (1.41)$$

**Fig. 1.18** The spin echo experiment [18]



Since the density matrix is continuous when the RF-field is switched on,  $\rho_R(0^-) = \rho_R(0^+)$ . During the RF-pulse  $\rho_R(t)$  is evolving as

$$\rho_R(t) = e^{\frac{i}{\hbar}\gamma H_1 t_x} \rho_R(0^-) e^{-\frac{i}{\hbar}\gamma H_1 t_x} \quad (1.42)$$

Here it is assumed that the frequency of  $H_1$  is so close to the resonance that the only contribution to  $H_{eff}$  is from the RF-field. In the previous section it was shown that when  $\gamma H_1 t_1 = \frac{\pi}{2}$  the net magnetization is flipped into the xy-plane. After the application of the first RF-pulse the spin system will evolve according to the solution with a time independent Hamiltonian  $H_{eff}$  in the rotating frame of reference.

$$\rho_R(t) = e^{i(\gamma H_0 - \omega)(t-t_1)I_z} \rho_R(t_1) e^{-i(\gamma H_0 - \omega)(t-t_1)I_z} \quad (1.43)$$

Applying a RF-pulse at  $t = t_2$  with a duration such that  $\gamma H_1(t_3 - t_2) = \pi$  the evolution of the density matrix at  $t > t_3$  is written

$$\rho_R(t) = e^{i\pi I_x - i(\gamma H_0 - \omega)(t-t_3)I_z} \rho_R(t_2) e^{i(\gamma H_0 - \omega)(t-t_3)I_z - i\pi I_x} \quad (1.44)$$

where  $\rho_R(t_2) = e^{i(\gamma H_0 - \omega)(t_2-t_1)I_z} \rho_R(t_1) e^{-i(\gamma H_0 - \omega)(t_2-t_1)I_z}$ . From (1.44) it can be seen that the effect of the last  $180^\circ$  RF-pulse is to change the sign in the exponents as compared with the evolution before the  $180^\circ$  RF-pulse. Thus, when assuming  $t_3 - t_2 \ll t_2 - t_1$ , the two parts will cancel at  $t = 2t_2$  and result in an echo that is independent of  $\gamma H_0 - \omega$

$$\rho_R(t = 2t_2) = e^{i\frac{3\pi}{2}I_x} \rho_R(0^-) e^{-i\frac{3\pi}{2}I_x} \quad (1.45)$$

Having found an expression for the density matrix an expression for the expectation value of the magnetization using the high temperature approximations ( $Z = 2I + 1$  and  $e^{-\gamma \hbar H_0 I_z / kT} \approx 1 - \frac{\gamma \hbar H_0 I_z}{kT}$ ) can be found

$$\langle M_y(2t_2) \rangle = \gamma \hbar \text{Tr} \{ \rho_R(2t_2) I_y \} = -\gamma^2 \hbar^2 H_0 \frac{NI(I+1)}{3kT} \quad (1.46)$$

Thus, all the initial magnetization following the first  $90^\circ$  RF-pulse has been refocused, i.e. a spin echo signal has been produced.

### ***The Response to a Pulsed Field Gradient Spin Echo Experiment***

In order to describe a pulsed field gradient spin echo experiment, it is necessary to include magnetic field gradients into the equations described in the previous

section. It is convenient to start with a small volume, calculate the density matrix through all the durations in the pulse sequence (as the Hamiltonian varies depending on on/offset of RF- and gradient pulses) and thereafter conduct the integration over the volume of interest. The probability that a particle which is initially at a position  $z_0$  at  $t = 0$  moves to a position at time  $\tau$  is given by the factor  $p(z_0)P(z, z_0, \tau)$ . This is a so called Markov process [48]; the experiment is insensitive to what happens between  $t = 0$  and  $t = \tau$ . Only the probability  $p(z_0)$  at  $t = 0$  and the probability  $P(z, z_0, \tau)$  at  $t = \tau$  will affect the experimental outcome.

When the time evolution of the magnetization of the spins is taken into account, the probability factor should be multiplied by the expectation value for the magnetization of the spins. This is equivalent to evaluating the expectation value for the magnetization of the particles that move during the pulsed field gradient spin echo experiment

$$\langle M_{xy}(2\tau) \rangle = \int \int p(z_0)P(z, z_0, \tau) \gamma \hbar \text{Tr} \{ \rho_R(2\tau) I_{xy} \} dz dz_0 \quad (1.47)$$

Using the result from the spin echo experiment and introducing a magnetic field gradient in the z-direction into the Hamiltonian,  $H_z = H_0 + gz$ , it may be shown that the density matrix at the time of the spin echo is written

$$\rho_R(2\tau) = -e^{iI_z \gamma \delta g(z(\tau) - z_0) + i\frac{\pi}{2} I_x} \rho_R(0^-) e^{-i\frac{\pi}{2} I_x - iI_z \gamma \delta g(z(\tau) - z_0)} \quad (1.48)$$

The major assumption used is that the spins do not move in the direction of the magnetic field gradient during the gradient pulse. The well known  $\delta/3$  correction to the diffusion time  $\tau$ , the duration between the gradient pulses, is then neglected. Again, using the commutator relations and the high temperature approximation,  $\rho_R$  can be written

$$\rho_R(2\tau) = \text{Constant} - \frac{\gamma \hbar H_0}{(2I + 1)kT} (I_x \cos(\gamma \delta g(z(\tau) - z_0)) + I_y \sin(\gamma \delta g(z(\tau) - z_0))) \quad (1.49)$$

Letting the x-component of the magnetization be the real part and the y-component the imaginary part, the expectation value for the magnetization of moving spins at  $t = 2\tau$  is then written

$$\langle M(2\tau) \rangle = M_0 \int \int p(z_0)P(z, z_0, \tau) e^{i\gamma \delta g(z(\tau) - z_0)} dz dz_0 \quad (1.50)$$

where

$$M_0 = -\gamma^2 \hbar^2 H_0 \frac{NI(I + 1)}{3kT} \quad (1.51)$$

To solve the integrals in (1.50) knowledge about how the spins move must be used. That is, the solution of the differential equation called Fick's law must be found. For a homogeneous system it is shown in Chap. 2 that  $p(z_0)P(z, z_0, \tau)$  is

Gaussian and (1.50) then yields the second order moment with respect to the magnetic field gradient

$$\langle M(2\tau) \rangle = M_0 e^{-\gamma^2 \delta^2 g^2 D \tau} \quad (1.52)$$

$D$  is the diffusion coefficient for the nuclear spins, and  $\tau$  is the duration between the gradient pulses.

### *Coherence Transfer Pathways and Effective Gradients*

When applying more than two RF-pulses in any pulse sequence, several echoes may be generated [18]. For example, in the ordinary pulsed field gradient stimulated echo experiment where three  $90^\circ$  RF-pulses are applied, five echoes will appear together with the FID's following each RF-pulse [34]. As the stimulated echo is the echo required in this sequence, the remaining echoes should be suppressed. A way to do this is to employ the concept of coherence transfer pathways aiming at constructing a phase sequence where the only surviving signal is the stimulated echo [49]. The coherence transfer pathway is given by

$$\varphi = \sum_{j=1}^n \Delta p_j \varphi_j \quad (1.53)$$

where  $\varphi$  is the accumulated phase change determined by the product of the change in coherence order  $\Delta p_j$  and the phase  $\varphi_j$  of the RF-pulse number  $j$ .  $n$  equals the number of RF-pulses applied in the experiment. The coherence order is dependent on the transitions possible within the spin system, and to the lowest order (non-interacting spin  $1/2$ ) one may define the coherence order  $p = 0$  in the direction of the external field and  $p = \pm 1$  transverse to it. A single spin initially at thermal equilibrium with the external field, will after the application of a  $90^\circ$  RF-pulse change the coherence level to  $+1$  (rotating clockwise in the plane transverse to the external field),  $-1$  (rotating counterclockwise), or it may be unaffected by the RF-pulse (i.e. coherence order 0). The  $\pm 1$  coherence levels are the two solutions for the transverse magnetization in the Bloch-Torrey equations. For the phase of the RF-pulses there are four possibilities;  $0$ ,  $\frac{\pi}{2}$ ,  $\pi$  and  $\frac{3\pi}{2}$ . In the rotating coordinate system this implies that the RF-pulse is applied in the  $\pm x$  or  $\pm y$  direction.

As an example, the coherence transfer pathway from the spin echo sequence is to be considered. A phase sequence is to be constructed, such that the only surviving signal is the one following the coherence order pathway  $p \rightarrow 0 \rightarrow -1 \rightarrow +1$ , shown in Fig. 1.19 as the solid line.

For the first scan, let the phases of the RF-pulses equal 0. Then the resulting phases for the different pathways are written as follows

$$\varphi = -1 \cdot 0 + 2 \cdot 0 = 0 \quad \text{and} \quad \varphi' = +1 \cdot 0 + 0 \cdot 0 = 0 \quad (1.54)$$

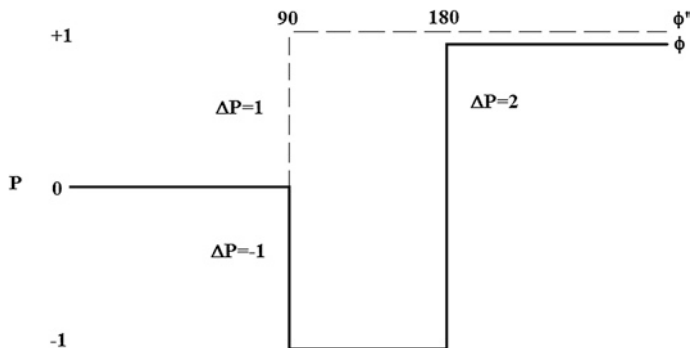


**Fig. 1.19** Coherence order pathway for spin echo sequence (also equivalent to the read interval in the 13-interval PFGSTE sequence)

For the second scan let the phase of the  $90^\circ$  RF-pulse be shifted by  $\frac{\pi}{2}$  while keeping the phase of the  $180^\circ$  RF-pulse unchanged. Then the resulting phases for the different pathways are written as follows

$$\varphi = -1 \cdot \frac{\pi}{2} + 2 \cdot 0 = -\frac{\pi}{2} \quad \text{and} \quad \varphi' = +1 \cdot \frac{\pi}{2} + 0 \cdot 0 = \frac{\pi}{2} \quad (1.55)$$

If the receiver phase is set to 0 and  $-\frac{\pi}{2}$ , and the two scans are added, the proposed phase sequence will result in a signal where the only contribution (ideally) is from the desired coherence transfer pathway  $p \rightarrow 0 \rightarrow -1 \rightarrow +1$ .

Finally, the concept of effective gradients is closely connected to the coherence transfer pathway. Karlicek et al. [1] showed using the Bloch-Torrey equations that the application of a  $180^\circ$  RF-pulse is equivalent to changing the polarity of the magnetic field gradient acting on the spin system. This can be seen using the concept of the density matrix: Consider the PFGSE in Fig. 1.3. The sequence yields an echo at  $t = 2\tau$  with two positive, apparently dephasing magnetic field gradients. How is it then possible to acquire an echo at  $t = 2\tau$ ? The mechanism for echo formation can be understood by examining the action of the  $180^\circ$  RF pulse on the transverse magnetization. The effect of this pulse is to change the coherence order from  $+1$  to  $-1$  (and vice versa), and (1.48) shows the resulting density matrix at  $t = 2\tau$ . When evaluating the resulting density matrix, it can be seen that the application of the  $180^\circ$  RF-pulse is equivalent to a change in the polarity of the effective magnetic field gradient. Thus, in the evaluation of the echo attenuation for more complicated PFGSTE sequences the  $180^\circ$  RF-pulse may be replaced by a change in sign of the magnetic field gradient following the RF-pulse.

***Mathematica Program for Solving the Echo Attenuation from the Ordinary Monopolar PFGSTE Sequence with Rectangular Shaped Gradients***

*Mathematica 5.1 program for evaluation of attenuation from ordinary PFGSTE (Fig. 1.5);*

```

h[x] = -G*x
i[x] = -G*x+g*(x-a)
j[x] = -G*x+g*(b-a)
n[x] = g*(b-a)-G*c
o[x] = G*(x-(2*c+d))+g*(b-a)
p[x] = G*(x-(2*c+d))+g*(b-a)-g*(x-(c+d+a))
q[x] = G*(x-(2*c+d))

h1[x] = h[x]^2
i1[x] = i[x]^2
j1[x] = j[x]^2
n1[x] = n[x]^2
o1[x] = o[x]^2
p1[x] = p[x]^2
q1[x] = q[x]^2

h2[x] = Integrate[h1[x],]
i2[x] = Integrate[i1[x],]
j2[x] = Integrate[j1[x],]
n2[x] = Integrate[n1[x],{x,c,c+d}]
o2[x] = Integrate[o1[x],{x,c+d,c+d+a}]
p2[x] = Integrate[p1[x],{x,c+d+a,c+d+b}]
q2[x] = Integrate[q1[x],{x,c+d+b,2*c+d}]

sum1[x] = h2[x]+i2[x]+j2[x]
sum2[x] = n2[x]+o2[x]+p2[x]+q2[x]
sum5[x] = sum1[x]+sum2[x]
sum5[x] = Simplify[sum5[x]]
X1[x] = Coefficient[sum5[x],g^2]*g^2
sum5[x] = sum5[x]-X1[x]
sum5[x] = Simplify[sum5[x]]
X3[x] = Coefficient[sum5[x],G^2]*G^2
sum5[x] = sum5[x]-X3[x]
sum5[x] = Simplify[sum5[x]]
X1[x] = Simplify[X1[x]]
X3[x] = Simplify[X3[x]]
X4[x] = Coefficient[sum5[x],G,1]*G
Result[x]=X1[x]+X3[x]+X4[x]

```

## ***Mathematica Programs for Solving the Echo Attenuation from the 13-Interval PFGSTE Sequence with Sinusoidal Gradients***

*Mathematica 5.1 program for evaluation of attenuation from the 13-PFGSTE (Fig. 1.20) using  $f=g$ ;*

```

h[x] = G*x
i[x] = G*x - g*((b-a)/Pi)*(Cos[Pi*(x-a)/(b-a)] - 1)
j[x] = G*x + (2/Pi)*g*(b-a)
k[x] = -G*(x-2c) + (2/Pi)*g*(b-a)
l[x] = -G*(x-2c) + (2/Pi)*g*(b-a) - g*((b-a)/Pi)*(Cos[Pi*(x-(c+a))/(b-a)] - 1)
m[x] = -G*(x-2c) + (4/Pi)*g*(b-a)
n[x] = (4/Pi)*g*(b-a)
o[x] = -G*(x-(2c+d)) + (4/Pi)*g*(b-a)
p[x] = -G*(x-(2c+d)) + (4/Pi)*g*(b-a) + g*((b-a)/Pi)*(Cos[Pi*(x-(2c+d+a))/(b-a)] - 1)
q[x] = -G*(x-(2c+d)) + (2/Pi)*g*(b-a)
r[x] = G*(x-(4c+d)) + (2/Pi)*g*(b-a)
s[x] = G*(x-(4c+d)) + (2/Pi)*g*(b-a) + (g*(b-a)/Pi)*(Cos[Pi*(x-(3c+d+a))/(b-a)] - 1)
t[x] = G*(x-(4c+d))

```

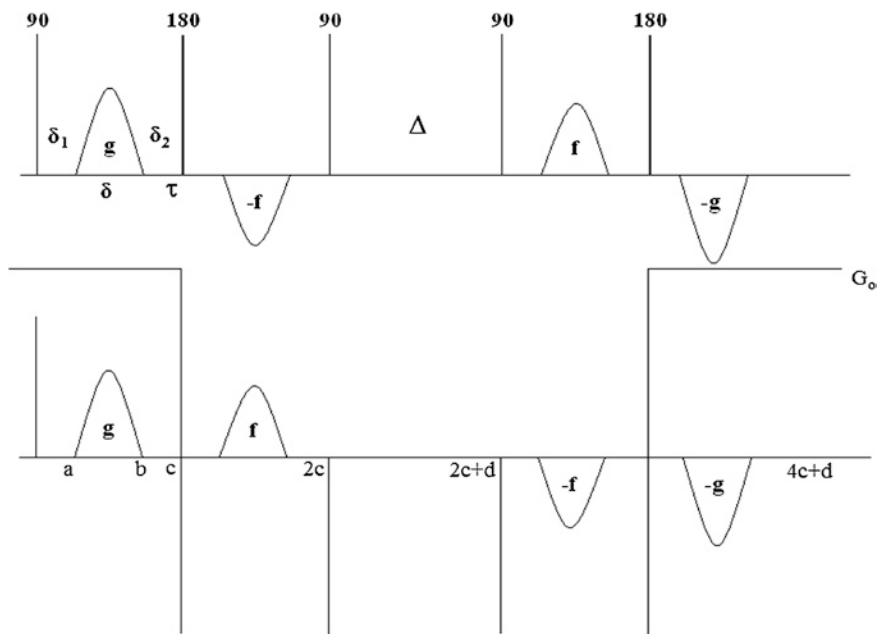


**Fig. 1.20** The 13-interval PFGSTE sequence with sinusoidal shaped gradients



$$h1[x] = h[x]^2$$

$$i1[x] = i[x]^2$$

$$j1[x] = j[x]^2$$

$$k1[x] = k[x]^2$$

$$l1[x] = l[x]^2$$

$$m1[x] = m[x]^2$$

$$n1[x] = n[x]^2$$

$$o1[x] = o[x]^2$$

$$p1[x] = p[x]^2$$

$$q1[x] = q[x]^2$$

$$r1[x] = r[x]^2$$

$$s1[x] = s[x]^2$$

$$t1[x] = t[x]^2$$

$$h2[x] = \text{Integrate}[h1[x], \{x, 0, a\}]$$

$$i2[x] = \text{Integrate}[i1[x], \{x, a, b\}]$$

$$j2[x] = \text{Integrate}[j1[x], \{x, b, c\}]$$

$$k2[x] = \text{Integrate}[k1[x], \{x, c, c+a\}]$$

$$l2[x] = \text{Integrate}[l1[x], \{x, c+a, c+b\}]$$

$$m2[x] = \text{Integrate}[m1[x], \{x, c+b, 2c\}]$$

$$n2[x] = \text{Integrate}[n1[x], \{x, 2c, 2c+d\}]$$

$$o2[x] = \text{Integrate}[o1[x], \{x, 2c+d, 2c+d+a\}]$$

$$p2[x] = \text{Integrate}[p1[x], \{x, 2c+d+a, 2c+d+b\}]$$

$$q2[x] = \text{Integrate}[q1[x], \{x, 2c+d+b, 3c+d\}]$$

$$r2[x] = \text{Integrate}[r1[x], \{x, 3c+d, 3c+d+a\}]$$

$$s2[x] = \text{Integrate}[s1[x], \{x, 3c+d+a, 3c+d+b\}]$$

$$t2[x] = \text{Integrate}[t1[x], \{x, 3c+d+b, 4c+d\}]$$

$$\text{sum1}[x] = h2[x] + i2[x] + j2[x] + k2[x] + l2[x] + m2[x]$$

$$\text{sum2}[x] = n2[x] + o2[x] + p2[x] + q2[x] + r2[x] + s2[x] + t2[x]$$

$$\text{sum5}[x] = \text{sum1}[x] + \text{sum2}[x]$$

$$\text{sum5}[x] = \text{Simplify}[\text{sum5}[x]]$$

$$X1[x] = \text{Coefficient}[\text{sum5}[x], g^2] * g^2$$

$$\text{sum5}[x] = \text{sum5}[x] - X1[x]$$

$$\text{sum5}[x] = \text{Simplify}[\text{sum5}[x]]$$

$$X2[x] = \text{Coefficient}[\text{sum5}[x], G^2] * G^2$$

$$\text{sum5}[x] = \text{sum5}[x] - X2[x]$$

$$\text{sum5}[x] = \text{Simplify}[\text{sum5}[x]]$$

$$X3[x] = \text{Coefficient}[\text{sum5}[x], G, 1] * G$$

$$X1[x] = \text{Simplify}[X1[x]]$$

$$X2[x] = \text{Simplify}[X2[x]]$$

$$X3[x] = \text{Simplify}[X3[x]]$$

$$\text{Result}[x] = X1[x] + X2[x] + X3[x]$$

The equation from the sequence with sinusoidal shaped gradients is

$$I = I_0 e^{-\frac{4\tau}{T_2}} e^{-\gamma^2 g^2 \left(\frac{4\delta}{\pi}\right)^2 D \left[\Delta + \frac{3\tau}{2} - \delta/8\right] - \frac{\gamma^2 D 4\delta(\delta_1 - \delta_2)(\tau) g G_0}{\pi} - \frac{4\tau^3 G_0}{3}} \quad (1.56)$$

Even though the cross term vanishes only if  $(\delta_1 - \delta_2) = 0$ , it is significantly reduced as there is no  $\Delta$  dependency.

## References

1. R.F. Karlicek Jr., I.J. Lowe, A modified pulsed gradient technique for measuring diffusion in the presence of large background gradients. *J. Magn. Reson.* (1969) **37**(1), 75–91 (1980)
2. R.M. Cotts et al., Pulsed field gradient stimulated echo methods for improved NMR diffusion measurements in heterogeneous systems. *J. Magn. Reson.* (1969) **83**(2), 252–266 (1989)
3. A. Jerschow, N. Müller, 3D diffusion-ordered TOCSY for slowly diffusing molecules. *J. Magn. Reson. A* **123**(2), 222–225 (1996)
4. G.H. Sørlund, D. Aksnes, L. Gjørdaker, A pulsed field gradient spin-echo method for diffusion measurements in the presence of internal gradients. *J. Magn. Reson.* **137**(2), 397–401 (1999)
5. G.H. Sørlund, B. Hafskjold, O. Herstad, A stimulated-echo method for diffusion measurements in heterogeneous media using pulsed field gradients. *J. Magn. Reson.* **124**(1), 172–176 (1997)
6. G.H. Sørlund et al., Improved convection compensating pulsed field gradient spin-echo and stimulated-echo methods. *J. Magn. Reson.* **142**(2), 323–325 (2000)
7. R. Blinc, J. Pirš, I. Zupančič, Measurement of self-diffusion in liquid crystals by a multiple-pulse NMR method. *Phys. Rev. Lett.* **30**(12), 546–549 (1973)
8. A. Jerschow, N. Müller, Convection compensation in gradient enhanced nuclear magnetic resonance spectroscopy. *J. Magn. Reson.* **132**(1), 13–18 (1998)
9. C.S. Johnson Jr, Diffusion ordered nuclear magnetic resonance spectroscopy: principles and applications. *Prog. Nucl. Magn. Reson. Spectrosc.* **34**(3–4), 203–256 (1999)
10. N.M. Loening, J. Keeler, G.A. Morris, One-dimensional DOSY. *J. Magn. Reson.* **153**(1), 103–112 (2001)
11. G.A. Morris, H. Barjat, Chapter 11 high resolution diffusion ordered spectroscopy, in *Analytical Spectroscopy Library*, ed. by K.E. Kévé, Gy. Batta, Cs. Széntay (Elsevier, 1997), pp. 209–226
12. M. Nilsson, G.A. Morris, Improving pulse sequences for 3D DOSY: convection compensation. *J. Magn. Reson.* **177**(2), 203–211 (2005)
13. A. Botana et al., J-modulation effects in DOSY experiments and their suppression: the Oneshot45 experiment. *J. Magn. Reson.* **208**(2), 270–278 (2011)
14. Y.Q. Song, M.D. Hürlimann, C. Flaum, A method for rapid characterization of diffusion. *J. Magn. Reson.* **161**(2), 222–233 (2003)
15. J.P. Stamps et al., Difftrain: a novel approach to a true spectroscopic single-scan diffusion measurement. *J. Magn. Reson.* **151**(1), 28–31 (2001)
16. S.J. Gibbs, C.S. Johnson Jr., A PFG NMR experiment for accurate diffusion and flow studies in the presence of eddy currents. *J. Magn. Reson.* (1969) **93**(2), 395–402 (1991)
17. G.H. Sørlund, D. Aksnes, L. Gjørdaker, A pulsed field gradient spin-echo method for diffusion measurements in the presence of internal gradients. *J. Magn. Reson.* **137**(2), 397–401 (1999)
18. E.L. Hahn, Spin echoes. *Phys. Rev.* **80**(4), 580–594 (1950)
19. A. Abragam, *The Principles of Nuclear Magnetism* (Oxford University Press, 1983), p. 618
20. F. Bloch, W.W. Hansen, M. Packard, Nuclear induction. *Phys. Rev.* **69**(3–4), 127 (1946)
21. C.P. Slichter, *Principles of Magnetic Resonance* (3rd enlarged and updated edition, Springer, 1990)
22. H.C. Torrey, Bloch equations with diffusion terms. *Phys. Rev.* **104**(3), 563–565 (1956)

23. J. Kärger, W. Heink, The propagator representation of molecular transport in microporous crystallites. *J. Magn. Reson.* (1969) **51**(1), 1–7 (1983)
24. L.L. Latour et al., Pore-size distributions and tortuosity in heterogeneous porous media. *J. Magn. Reson. A* **112**(1), 83–91 (1995)
25. L.L. Latour et al., Time-dependent diffusion coefficient of fluids in porous media as a probe of surface-to-volume ratio. *J. Magn. Reson. A* **101**(3), 342–346 (1993)
26. R.W. Mair et al., Probing porous media with gas diffusion NMR. *Phys. Rev. Lett.* **83**(16), 3324–3327 (1999)
27. P.P. Mitra, P.N. Sen, L.M. Schwartz, Short-time behavior of the diffusion coefficient as a geometrical probe of porous media. *Phys. Rev. B* **47**(14), 8565–8574 (1993)
28. P.P. Mitra, B.I. Halperin, Effects of finite gradient-pulse widths in pulsed-field-gradient diffusion measurements. *J. Magn. Reson. A* **113**(1), 94–101 (1995)
29. P.P. Mitra et al., Diffusion propagator as a probe of the structure of porous media. *Phys. Rev. Lett.* **68**(24), 3555–3558 (1992)
30. K.E. Washburn, C.H. Arns, P.T. Callaghan, Pore characterization through propagator-resolved transverse relaxation exchange. *Phys. Rev. E* **77**(5), 051203 (2008)
31. R.L. Kleinberg, W.E. Kenyon, P.P. Mitra, Mechanism of NMR relaxation of fluids in rock. *J. Magn. Reson. A* **108**(2), 206–214 (1994)
32. S. Godefroy, P.T. Callaghan, 2D relaxation/diffusion correlations in porous media. *Magn. Reson. Imaging* **21**(3–4), 381–383 (2003)
33. E.O. Stejskal, J.E. Tanner, Spin diffusion measurements: spin echoes in the presence of a time-dependent field gradient. *J. Chem. Phys.* **42**(1), 288–292 (1965)
34. J.M. Fauth et al., Elimination of unwanted echoes and reduction of dead time in three-pulse electron spin-echo spectroscopy. *J. Magn. Reson.* (1969), **66**(1), 74–85 (1986)
35. L.E. Drain, The broadening of magnetic resonance lines due to field inhomogeneities in powdered samples. *Proc. Phys. Soc.* **80**(6), 1380 (1962)
36. W. Heink et al., PFG NMR Self-diffusion measurements with large field gradients. *J. Magn. Reson. A* **114**(1), 101–104 (1995)
37. S. Meiboom, D. Gill, Modified spin-echo method for measuring nuclear relaxation times. *Rev. Sci. Instrum.* **29**(8), 688–691 (1958)
38. D.H. Wu, A.D. Chen, C.S. Johnson, An improved diffusion-ordered spectroscopy experiment incorporating bipolar-gradient pulses. *J. Magn. Reson. A* **115**(2), 260–264 (1995)
39. H.Y. Carr, E.M. Purcell, Effects of diffusion on free precession in nuclear magnetic resonance experiments. *Phys. Rev.* **94**(3), 630–638 (1954)
40. G.H. Sorland et al., Improved convection compensating pulsed field gradient spin-echo and stimulated-echo methods. *J. Magn. Reson.* **142**(2), 323–325 (2000)
41. G.H. Sørland, H.W. Anthonen, K. Zick, J. Sjöblom, A spoiler recovery method for rapid diffusion measurements. *Diffus. Fundam.* **15**, 9 (2011)
42. G.H. Sørland, Characterization of emulsions by PFG-NMR. *AIP Conf. Proc.* **1330**(1), 27–30 (2011)
43. V.V. Krishnan, N. Murali, Radiation damping in modern NMR experiments: progress and challenges. *Prog. Nucl. Magn. Reson. Spectrosc.* **68**, 41–57 (2013)
44. H.W. Anthonen, G.H. Sørland, K. Zick, J. Sjöblom, Quantitative recovery ordered (Q-ROSY) and diffusion ordered spectroscopy using the spoiler recovery approach. *Diffus. Fundam.* **16**, 12 (2012)
45. T. Stait-Gardner, P.G. Anil, W.S. Price, Steady state effects in PGSE NMR diffusion experiments. *Chem. Phys. Lett.* **462**(4–6), 331–336 (2008)
46. J. Mitchell, M.D. Hürlimann, E.J. Fordham, A rapid measurement of T1/T2: the DECPMG sequence. *J. Magn. Reson.* **200**(2), 198–206 (2009)
47. L. Venturi, K. Wright, B. Hills, Ultrafast T1–T2 relaxometry using FLOP sequences. *J. Magn. Reson.* **205**(2), 224–234 (2010)
48. R. Durrett, *Probability Theory and Examples* (4th ed, Cambridge University Press, 2010), p. 438
49. A.D. Bain, Coherence levels and coherence pathways in NMR. A simple way to design phase cycling procedures. *J. Magn. Reson.* (1969) **56**(3), 418–427 (1984)

<http://www.springer.com/978-3-662-44499-3>

Dynamic Pulsed-Field-Gradient NMR

Sorland, G.H.

2014, XIII, 354 p. 257 illus., 79 illus. in color., Hardcover

ISBN: 978-3-662-44499-3